Article:

Ye, H and Liu, R orcid.org/0000-0003-0627-3184 (2017) Nonlinear programming methods based on closed-form expressions for optimal train control. Transportation Research Part C: Emerging Technologies, 82. pp. 102-123. ISSN 0968-090X

https://doi.org/10.1016/j.trc.2017.06.011

Please cite this article as: "Ye, H., Liu, R., 2017. Nonlinear programming methods based on closed-form expressions for optimal train control. Transportation Research Part C 82, 102-123."

Nonlinear programming methods based on closed-form expressions for optimal train control

Hongbo Ye and Ronghui Liu*

Institute for Transport Studies, University of Leeds, Leeds, LS2 9JT, United Kingdom

Abstract

This paper proposes a novel approach to solve the complex optimal train control problems that so far cannot be perfectly tackled by the existing methods, including the optimal control of a fleet of interacting trains, and the optimal train control involving scheduling. By dividing the track into subsections with constant speed limit and constant gradient, and assuming the train's running resistance to be a quadratic function of speed, two different methods are proposed to solve the problems of interest. The first method assumes an operation sequence of maximum traction – speedholding – coasting – maximum braking on each subsection of the track. To maintain the mathematical tractability, the maximum tractive and maximum braking functions are restricted to be decreasing and piecewise-quadratic, based on which the terminal speed, travel distance and energy consumption of each operation can be calculated in a closed-form, given the initial speed and time duration of that operation. With these closed-form expressions, the optimal train control problem is formulated and solved as a nonlinear programming problem. To allow more flexible forms of maximum tractive and maximum braking forces, the second method applies a constant force on each subsection. Performance of these two methods is compared through a case study of the classic single-train control on a single journey. The proposed methods are further utilised to formulate more complex optimal train control problems, including scheduling a subway line while taking train control into account, and simultaneously optimising the control of a leader-follower train pair under fixed- and moving-block signalling systems.

Keywords: optimal train control; energy consumption; nonlinear programming; closed-form expression; subway line scheduling; simultaneous multi-train control

* Corresponding author. Tel.: +44 113 343 5338.
E-mail address: R.Liu@its.leeds.ac.uk (R. Liu).

1. Introduction

The traditional optimal train control problem is to find the energy-efficient strategy to drive the train through a specific railway segment within a predetermined time, while maintaining specific speeds at both ends of the segment. The problem is usually formulated as an optimal control problem, and solved to provide the train drivers with detailed speed or control advice along the segment[1].

The shape of the energy-efficient control/speed profile has been well studied with Pontryagin's maximum principle. The optimal train control strategy on level tracks with constant speed limit follows a sequence of (at most) four operations, which are maximum traction (MT), speedholding (SH), coasting (CS), and maximum braking (MB) (Asnis et al., 1985; Howlett, 1990; Ichikawa, 1968; Milroy, 1980). On undulating tracks with variable speed restrictions, these four operations can still compose the optimal control strategy (Albrecht et al., 2016a, 2016b; Howlett, 2000; Khmelnitsky, 2000; Liu and Golovitcher, 2003). State-of-the-art development on the optimal train control problem with continuous control is summarised by Albrecht et al. (2016a, 2016b), together with extension under more generalised assumptions. For trains with discrete control levels, the speedholding can be approximated by coast-power pairs (Cheng and Howlett, 1992, 1993; Cheng et al., 1999; Howlett, 1996; Howlett and Cheng, 1997; Pudney and Howlett, 1994). Comprehensive reviews of the analysis on classic single-train optimal control with continuous or discrete control can further be found in Scheepmaker et al. (2017) and Yang et al. (2016b).

Knowing the shape of the optimal control profile is not enough to drive the train in an energy-efficient way. The drivers need to be advised to take appropriate action at specific time or location of the journey, such as the speed to follow or the engine power to set. For this purpose, the optimal control problem has to be solved in order to generate the optimal control/speed profile along the journey (for reviews of the solution methods, see Scheepmaker et al., 2017; Yang et al., 2016b). Efficient algorithms have been developed based on the so-called indirect method, which tries to solve the Hamiltonian associated with the original optimal control problem based on Pontryagin's maximum principle (Albrecht et

[1] It is possible that the suggested control advice is not able to perfectly reproduce the desired optimal speed profile in a practical train run due to, e.g., the inter-carriage interaction which is not considered in the optimal train control problem. It leads to the so-called train "cruise control" problem which deals with how to follow a prescribed speed profile. We do not consider the cruise control in this paper but refer interested readers to Li et al. (2014, 2015) for it.

al., 2016a, 2016b; Howlett et al., 2009; Khmelnitsky, 2000; Liu and Golovitcher, 2003). Still, the indirect method cannot perfectly solve optimal train control in more complex settings, such as the optimal control of a fleet of trains, or the optimal train control with extra intermediate constraints applied on the train run, e.g., when the trains are required to dwell at the intermediate stations or to pass specific track locations within specific time windows. Alternatively, the optimal control formulations of these complex optimal train control problems can be first discretised by some numerical methods and then solved by mathematical programming techniques such as linear programming (Wang et al., 2013), nonlinear programing (Wang and Goverde, 2016a, 2016b, 2016c; Wang et al., 2013, 2014; Ye and Liu, 2016) and dynamic programming (Effati and Roohparvar, 2006; Franke et al., 2000; Ko et al., 2004; Vasak et al., 2009; Zhou et al., 2017). Quality of these discretisation-based methods depends on the discretisation step: a larger step-size requires less computation effort but yields larger energy cost and/or larger violation on the constraints. In addition, as one can find in Effati and Roohparvar (2006), Wang and Goverde (2016a) and Ye and Liu (2016), these discretisation-based methods would sometimes give fluctuating control/speed profiles which are difficult to follow or implement for the automatic train operation.

Besides the indirect methods, there are other methods built upon the pre-specified four operations. The driving plans based on coasting control (Açıkbaş and Söylemez, 2008; Chang and Sim, 1997; Wong and Ho, 2004) are easy to implement; however, their energy saving is restricted by the limited searching space and the pre-specified operation rules. Mathematical programming methods (Gu et al., 2014; Li and Lo, 2014a, 2014b; Yang et al., 2015) are developed in these years, which either require simplification on the train characteristics or track condition, such as constant maximum traction/braking force and/or zero running resistance, or rely on simulation to calculate the ordinary differential equations (ODEs) and integrals. Such simplification restricts the general application of these methods, for example, when the train speed is high such that the maximum traction/braking force is not able to maintain constant and the running resistance is not negligible; on the other hand, the simulation slows the solution process. Recently, Haahr et al. (2017) proposed a method based on dynamic programming. Forward and backward speed profiles were pre-generated under the four operations at prescribed discrete speed levels and at locations where the speed limit or gradient changes. Neither location nor time was discretised, so the fluctuating speed/control profiles were avoided. As only a limited number of discrete speed levels were considered, the prescribed journey time constraint could be slightly violated, and the minimum energy consumption obtained could be larger than the optimum when continuous speeds were considered.

In addition to the constraints at the two ends of a journey, the train control problem may sometimes involve intermediate constraints. For example, in Haahr et al. (2017) and Wang and Goverde (2016a, 2016c), the train needs to pass specific track locations within specific time/speed windows; in Ye and Liu (2016), the leading train is required to stop at the passing loop to let the following train overtake. The pseudospectral method (PM) has been used to solve these problems but it sometimes leads to undesired violent fluctuation on the control profiles (Wang and Goverde, 2016a; Ye and Liu, 2016). A dynamic-programming-based method recently developed by Haahr et al. (2017) appears to overcome such issue. The train control problems with intermediate constraints also include a large group of research on the energy-efficient subway line scheduling, where the train needs to run through the whole subway line while stopping at stations for passenger boarding and alighting (see Scheepmaker et al., 2017; Yang et al., 2016b for comprehensive reviews). To solve the subway line scheduling problems, previous literature usually assumed simplified train characteristics such as nil running resistance and constant maximum tractive/braking force, or relied on simulation/discretisation to calculate the speed, travel distance and energy consumption (Chevrier et al., 2013; Das Gupta et al., 2016; Li and Lo, 2014a, 2014b; Yang et al., 2015, 2016a; Yin et al., 2016; Zhou et al., 2017). Howlett (2016) recently pointed out that, when no speed restriction is imposed, the different interstation journeys should share a same optimal speed; however, there are still no effective methods to find either this optimal speed or the optimal interstation running times.

So far in this introductory part, we have been talking about the control of a single train. However, a train's optimal driving plan may be infeasible, or not optimal from the systematic point of view, when it is running close to other trains on the same track in the same direction. For instance, a following train may have to give up its optimal strategy in order to yield to the safe separation to the leading train; likewise, the leading train may also need to compromise its optimal driving plan for the advancing and energy saving of the following trains. Meanwhile, the trajectories of trains running in different directions can also conflict if they need to use the same piece of track at the same time (Wang and Goverde, 2016b). Therefore, the control optimisation of all the trains under consideration should be conducted in an aggregate manner. For such problems, the discretisation-based numerical methods (Wang and

Goverde, 2016a, 2016b, 2016c; Wang et al., 2014; Yan et al., 2016; Ye and Liu, 2016) and the coasting control (Açıkbaş and Söylemez, 2008; Goodwin et al., 2016; Lu and Feng, 2011; Yang et al., 2012) can still work; however, their shortcomings persist as in solving the classic single-train control problems. Alternatively, Albrecht et al. (2015) developed a method based on the four well-known operations to control a pair of leading and following trains in a fixed-block system with prescribed intermediate section clearance times, and provided the necessary condition for checking the optimality of the clearance times. However, their method requires further improvement, for example, in the generalisation on existing track settings of zero gradients and no speed restriction, and in the methodology for finding the optimal clearance times.

In summary, the single-train optimal control without intermediate constraints can be perfectly solved now, but not the more complex problems involving multiple trains and/or intermediate constraints; these complex problems are what we would like to explore in this paper. We propose to solve the optimal train control problem with pre-specified operation sequence and practical train and track settings. The maximum traction force, maximum braking force and the train running resistance are assumed to be functions of speed. The uneven track and variable speed limit are explicitly considered, where the track gradient and speed limit are assumed piecewise-constant, so the track can be divided into subsections such that each subsection is of constant gradient and constant speed limit. We propose two different methods to solve the single-train optimal control problem as the nonlinear programming (NLP) problems, and then extend these two methods for the more complex optimal train control. The first method restricts the maximum traction and maximum braking forces to be decreasing and piecewise-quadratic w.r.t. speed, and the running resistance to be quadratic w.r.t. speed. The control on each subsection is assumed to follow the sequence of MT-SH-CS-MB. Given the initial speed and time duration of each operation on each subsection, we can get the closed-form expressions of the terminal speed, distance traversed and energy consumed corresponding to this operation. An NLP formulation would then be used to obtain the time duration of each operation on each subsection. To allow more general forms of maximum traction and maximum braking forces, the second method applies constant tractive/braking force on each subsection and uses the similar technique to formulate the NLP problem. Performance of these two methods is compared by numerical examples. The two methods are further used to solve two complex optimal train control problems. The first problem embeds sophisticated train control in an energy-efficient subway line scheduling process. The second problem considers the optimal control of multiple trains in both fixed-block and moving-block signalling systems.

Contributions of this paper, in comparison with exiting literature, are highlighted as follows.

(I) We focus on offline train speed/control profile optimisation for complex optimal train control problems that cannot be solved by the indirect methods based on Pontryagin's maximum principle, such as those with train interaction and/or intermediate constraints.

(II) Compared with the existing methods that solve the complex optimal train control problems which we are interested in, the merits and advantages of our methods lie in that:

- (i) We allow (more) realistic train and track conditions, so the resultant control/speed profile is feasible and close to the true optimum;
- (ii) We can achieve better energy saving than coasting control, which is not unexpected since the performance of the latter is constrained by the coasting rules and the number of coasting operations;
- (iii) We can obtain highly applicable control profiles which apply at most four operations on each subsection, therefore avoid unrealistic fluctuation;
- (iv) The closed-form expressions of speed, distance and energy can help accelerate the solution process. As a result, although we are focusing on offline optimisation as stated in Point (I), our algorithms can run fast, as demonstrated in the case studies, which lends their potential for online optimisation in the future.

The rest of this paper is organised as follows. Section 2 reviews the classic optimal train control problem. To solve this problem, two NLP methods are proposed in Section 3. The proposed methods are then used in Section 4 to solve the energy-efficient subway line scheduling problem (Section 4.1) and the multi-train optimal control problem (Section 4.2), respectively. Section 5 demonstrates two case studies: one compares the performance of the two proposed methods as well as the PM in solving a classic optimal train control problem, and the other solves the subway line scheduling problem. Section 6 draws the conclusions and discusses the future research directions.

2. Classic optimal train control problem

We briefly review the classic optimal train control problem in this section. The movement of a point-mass train is described as (Jaekel and Albrecht, 2014; Rochard and Schmid, 2000):

$$\frac{dx}{dt} = v \tag{1}$$

$$\frac{dv}{dt} = \frac{1}{M}\left(F - R(v) - G(x)\right) \tag{2}$$

where $x = x(t)$ and $v = v(t)$ are respectively the train's location and speed at time t; M is the train mass; $F = F(t)$ is the instantaneous force applied to the train, positive for traction and negative for braking; $R(v)$ is the running resistance at speed v, consisting of mechanical and aerodynamic resistances; $G(x)$ is the component of the gravitational force along the track, i.e.,

$$G(x) = Mg\sin\left(\arctan\theta(x)\right) \approx Mg\theta(x) \tag{3}$$

where g is the gravitational constant, and $\theta(x)$ is the track gradient at location x, defined as the ratio of vertical rise to the horizontal displacement. The approximation in Eq. (3) holds when $\theta(x)$ is close to zero.

The train speed and applied force are bounded as follows,

$$0 \le v \le \bar{v}(x) \tag{4}$$

$$-\overline{B^r}(v) \le F \le \overline{T^r}(v) \tag{5}$$

where $\bar{v}(x)$ is the upper speed limit at location x; $\overline{T^r}(v)$ and $\overline{B^r}(v)$ are respectively the maximum tractive force and maximum braking force at speed v, both of which are nonnegative and decreasing w.r.t. v.

The goal of the optimal train control is then to drive a train from location X_0 to location X_f ($X_f > X_0$) within a time budget T, while using as little energy as possible. Assuming the energy is consumed when and only when the tractive force is applied, and no energy is regenerated from braking, then the optimal train control problem can be formulated as follows,

$$\min \int_0^T \max\left\{F(t), 0\right\} v(t)\, dt \tag{6}$$

s.t. Eqs. (1)-(5), and

$$x(0) = X_0, \quad x(T) = X_f, \quad v(0) = V_0, \quad v(T) = V_f \tag{7}$$

where V_0 and V_f are the prescribed speeds at locations X_0 and X_f, respectively.

We further make the following assumptions on the running resistance as well as speed limit and track gradient.

Assumption 1. The running resistance $R(v)$ follows the Davis formula (Davis, 1926):

$$R(v) = A_0 + A_1 v + A_2 v^2 \tag{8}$$

where A_0, A_1 and A_2 are train-specific constants. As explained in Davis (1926), A_0 comprises journal friction, rolling resistance and track resistance; $A_1 v$ contains mainly flange friction but also frictions caused by concussion, swaying and oscillation; $A_2 v^2$ represents the air resistance.

Assumption 2. Both the speed limit and track gradient are piecewise constant w.r.t. location. Therefore, we can divide the track segment $\left[X_0, X_f\right]$ into N subsections (which are sequentially numbered 1 to N along the train's moving direction), such that both the speed limit and gradient are constant on each subsection, i.e.,

$$\begin{cases} \theta(x) = \theta^{(n)} \\ \bar{v}(x) = \bar{v}^{(n)} \end{cases}, \quad x \in \left[X^{(n)}, X^{(n+1)}\right], \quad n = 1, 2, \cdots, N \tag{9}$$

where $X^{(n)}$ and $X^{(n+1)}$, $X^{(n+1)} > X^{(n)}$, are the locations of the two ends of subsection n, $X^{(1)} = X_0$ and $X^{(N+1)} = X_f$, and constants $\theta^{(n)}$ and $\bar{v}^{(n)}$ are the corresponding gradient and speed limit.

We call Eq. (9) a "subsection plan" (SP). In an SP, two adjacent subsections can be identical in both gradient and speed limit. An SP is called a "max-length SP" if it has no adjacent subsections identical in both gradient and speed limit. The max-length SP can be modified by subdividing the subsections according to a predetermined length $\bar{S}$ shown as follows. For a subsection n of length $S^{(n)} = X^{(n+1)} - X^{(n)}$, if $S^{(n)} > \bar{S}$, then it will be cut into $\lceil S^{(n)}/\bar{S} \rceil$ subsections of equal length, where $\lceil S^{(n)}/\bar{S} \rceil$ is the smallest integer no smaller than $S^{(n)}/\bar{S}$. As a result, the subsection lengths in the modified SP will be at most $\bar{S}$.

3. Nonlinear programming methods for solving the classic optimal train control problem

In this section, we solve the general optimal train control problem (1)-(9) by converting it into the NLP problems. More specifically, we solve ODEs (1)-(2) and integral (6) analytically and obtain the closed-form expressions of speed, location and energy consumption. Consequently, Eqs. (1), (2) and (6) are replaced by these closed-form expressions, and the optimal control problem (1)-(9) is converted into NLP problems. Two different methods based on two different control strategies will be presented subsequently, which are respectively the four-stage strategy and the constant-force strategy.

3.1. Method 1: four-stage strategy

We first consider the optimal train control on a particular subsection n with constant speed limit $\bar{v}^{(n)}$ and constant gradient $\theta^{(n)}$. According to existing research, the train can be controlled in an energy-efficient way by sequentially applying the four operations (or say stages) of MT, SH, CS and MB. The force applied in each stage is given as follows,

$$F = \begin{cases} \overline{T^r}(v) & \text{MT} \\ R(v) + Mg\theta^{(n)} & \text{SH} \\ 0 & \text{CS} \\ -\overline{B^r}(v) & \text{MB} \end{cases} \tag{10}$$

where $Mg\theta^{(n)}$ is constant and $R(v)$ is a quadratic function of v given in Eq. (8). Notably, a speed of v can be held if and only if $-\overline{B^r} \le R(v) + Mg\theta^{(n)} \le \overline{T^r}$. Substituting Eq. (10) into the speed dynamic (2), we have

$$\frac{dv}{dt}=\begin{cases}\overline{T^r}-R(v)-Mg\theta^{(n)} & MT\\ 0 & SH\\ -R(v)-Mg\theta^{(n)} & CS\\ -\overline{B^r}-R(v)-Mg\theta^{(n)} & MB\end{cases} \tag{11}$$

To calculate the closed-form expressions of speed, location and energy consumption w.r.t. each operation, we first make the following assumption on the forms of maximum tractive and maximum braking forces.

Assumption 3. The maximum tractive force and maximum braking force are both decreasing and piecewise-linear w.r.t. speed, with at most two pieces, i.e.,

$$\overline{T^r}(v)=\begin{cases}\alpha_1 v+\beta_1, & 0\le v\le v_a\\ \alpha_2 v+\beta_2, & v>v_a\end{cases},\quad \alpha_1\le 0,\ \alpha_2\le 0,\ \beta_1\ge 0,\ \beta_2\ge 0, \alpha_1 v_a+\beta_1\ge\alpha_2 v_a+\beta_2 \tag{12}$$

and

$$\overline{B^r}(v)=\begin{cases}\lambda_1 v+\xi_1, & 0\le v\le v_b\\ \lambda_2 v+\xi_2, & v>v_b\end{cases},\quad \lambda_1\le 0,\ \lambda_2\le 0,\ \xi_1\ge 0,\ \xi_2\ge 0,\ \lambda_1 v_b+\xi_1\ge\lambda_2 v_b+\xi_2 \tag{13}$$

Some possible shapes of $\overline{T^r}(v)$ and $\overline{B^r}(v)$ are illustrated in Figure 1 (Figure 1(a) for a continuous form and Figure 1(b) for a discontinuous form), where v^c is the critical speed at which the maximum tractive/braking force function switches from one piece to the other, i.e. $v^c=v_a$ for MT and $v^c=v_b$ for MB. The pieces with speed lower and higher than v^c are respectively called Regime 1 and Regime 2.

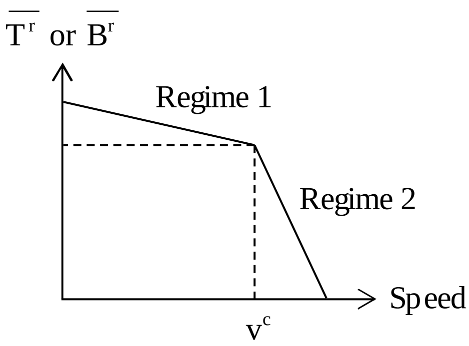

(a) Example of a continuous form

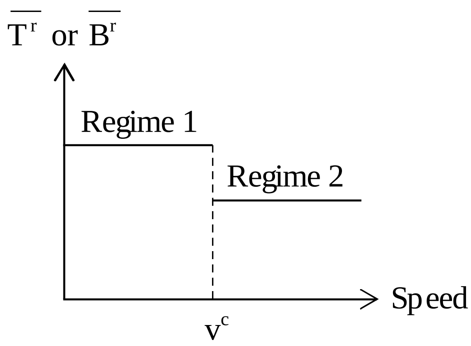

(b) Example of a discontinuous form

Figure 1. Examples of maximum tractive and maximum braking forces.

Remark 1. The forms of $\overline{T^r}(v)$ and $\overline{B^r}(v)$ that are allowed under the four-stage strategy could be more complex than that assumed in Assumption 3, which could be piecewise-quadratic of arbitrarily many pieces. However, considering a more complex form would not introduce extra difficulty in modelling but only extra complexity in calculating the closed-form expressions. Specifically, including the quadratic term requires calculating the integral of cube of speed w.r.t. time for obtaining the energy consumption (see Eq. (17)), while allowing more pieces would complicate the discussion of switching condition in Appendix B for calculating the closed-form expressions w.r.t. the MT and MB stages. □

Remark 2. When considering non-constant $\overline{T^r}(v)$ and $\overline{B^r}(v)$, the literature usually assumes forms more general than piecewise-linear and piecewise-quadratic. We can approximate the nonlinear piece(s) by the piecewise-linear function, as shown in the following Figure 2. We suggest using tangent lines rather secant lines so that the obtained control profile will always be feasible. □

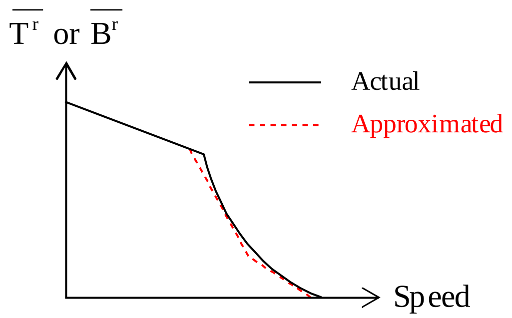

Figure 2. Approximation of a piecewise-nonlinear maximum tractive/braking function.

Substituting Eqs. (12) and (13) into Eq. (11) further reads

$$\frac{dv}{dt}=\begin{cases}\left.\begin{array}{ll}\alpha_1 v+\beta_1-R(v)-Mg\theta^{(n)} & 0\le v\le v_a\\ \alpha_2 v+\beta_2-R(v)-Mg\theta^{(n)} & v>v_a\end{array}\right\} & \text{MT}\\ 0 & \text{SH}\\ \qquad -R(v)-Mg\theta^{(n)} & \text{CS}\\ \left.\begin{array}{ll}-\lambda_1 v-\xi_1-R(v)-Mg\theta^{(n)} & 0\le v\le v_b\\ -\lambda_2 v-\xi_2-R(v)-Mg\theta^{(n)} & v>v_b\end{array}\right\} & \text{MB}\end{cases} \tag{14}$$

Since $R(v)$ is quadratic, the six ODEs in Eq. (14) can be expressed in a unified form

$$\frac{dv}{dt} = av^2 + bv + c \tag{15}$$

but with different values of a, b and c. The closed-form solution of Eq. (15) is calculated in Appendix A. Notably, during a MT (MB) stage, the speed is monotonically changing with time (proved in Appendix B), so the maximum tractive (braking) force may switch from one regime to the other. In this case, the closed-form expression of $v(t)$ could be a piecewise function, which is discussed in detail in Appendix B.

To solve the optimal train control problem (1)-(9), we adopt the four-stage strategy on each subsection. Notably, one can skip certain stages by assigning zero time duration to them. For a particular subsection n, let $v_0^{(n)}$ be the initial speed on it, and $v_i^{(n)}$ and $\tau_i^{(n)}$ respectively be the terminal speed and duration of stage i ($i=1$ for MT, $i=2$ for SH, $i=3$ for CS, and $i=4$ for MB). Also, let $\phi_i\left(v_{i-1}^{(n)}, \tau_i^{(n)}, \theta^{(n)}\right)$ and $s_i\left(v_{i-1}^{(n)}, \tau_i^{(n)}, \theta^{(n)}\right)$ respectively be the functions of terminal speed and distance traversed of stage i, given initial speed $v_{i-1}^{(n)}$, time duration $\tau_i^{(n)}$ and gradient $\theta^{(n)}$. Then for SH, we have $\phi_2\left(v_1^{(n)}, \tau_2^{(n)}, \theta^{(n)}\right) = v_1^{(n)}$ and $s_2\left(v_1^{(n)}, \tau_2^{(n)}, \theta^{(n)}\right) = v_1^{(n)}\tau_2^{(n)}$; for the other three stages (MT, CS, MB), the closed-form expressions of these two functions can be calculated according to Appendix A and Appendix B. For energy consumption, denote $E_i\left(v_{i-1}^{(n)}, \tau_i^{(n)}, \theta^{(n)}\right)$ as the energy consumed during stage i on subsection n, where $i=1,2$ since only the MT and SH stages are possible to consume energy. For the SH stage,

$$E_2\left(v_1^{(n)}, \tau_2^{(n)}, \theta^{(n)}\right) = v_1^{(n)}\tau_2^{(n)} \max\left\{0, R\left(v_1^{(n)}\right) + Mg\theta^{(n)}\right\} \tag{16}$$

For the MT stage, if the maximum tractive force keeps in a particular Regime k, $k=1,2$, then let $T_0^{(n)} = \sum_{j=1}^{n-1}\sum_{i=1}^{4}\tau_i^{(j)}$ be the time of entering subsection n and we have

$$\begin{aligned} E_1\left(v_0^{(n)}, \tau_1^{(n)}, \theta^{(n)}\right) &= \int_{T_0^{(n)}}^{T_0^{(n)}+\tau_1^{(n)}} \left(\alpha_k v(t) + \beta_k\right) v(t)\, dt \\ &= \beta_k s_1\left(v_0^{(n)}, \tau_1^{(n)}, \theta^{(n)}\right) + \alpha_k \int_{T_0^{(n)}}^{T_0^{(n)}+\tau_1^{(n)}} \left(v(t)\right)^2 dt \end{aligned} \tag{17}$$

The closed-form expression of the second integral in Eq. (17) is provided in Appendix A. If the maximum tractive force switches from one regime to the other during the MT stage, then the switching condition discussed in Appendix B should be considered when calculating $E_1\left(v_0^{(n)}, \tau_1^{(n)}, \theta^{(n)}\right)$.

The optimal train control problem (1)-(9) is then formulated as the following NLP problem.

$$\min_{\left\{v_i^{(n)}, \tau_i^{(n)}\right\}} \sum_{n=1}^{N} \sum_{i=1}^{2} E_i\left(v_{i-1}^{(n)}, \tau_i^{(n)}, \theta^{(n)}\right) \tag{18}$$

$$\text{s.t.} \quad v_i^{(n)} = \phi_i\left(v_{i-1}^{(n)}, \tau_i^{(n)}, \theta^{(n)}\right), \ \ i = 1, 2, 3, 4, \ \ n = 1, 2, \cdots, N \tag{19}$$

$$v_0^{(n)} = v_4^{(n-1)}, \ \ n = 2, 3, \cdots, N \tag{20}$$

$$v_0^{(1)} = V_0, \ \ v_4^{(N)} = V_f \tag{21}$$

$$0 \le v_i^{(n)} \le \overline{v}^{(n)}, \ \ i = 0, 1, 2, 3, \ \ n = 1, 2, \cdots, N \tag{22}$$

$$\sum_{n=1}^{N} \sum_{i=1}^{4} \tau_i^{(n)} = T \tag{23}$$

$$0 \le \tau_i^{(n)} \le T - \sum_{k=1, k \ne n}^{N} \frac{S^{(k)}}{\overline{v}^{(k)}}, \ \ i = 1, 2, 3, 4, \ \ n = 1, 2, \cdots, N \tag{24}$$

$$\sum_{i=1}^{4} s_i\left(v_{i-1}^{(n)}, \tau_i^{(n)}, \theta^{(n)}\right) = S^{(n)}, \ \ n = 1, 2, \cdots, N \tag{25}$$

$$\tau_2^{(n)}\left[R\left(v_1^{(n)}\right) + Mg\theta^{(n)} + \overline{B^r}\left(v_1^{(n)}\right)\right] \ge 0, \ \ n = 1, 2, \cdots, N \tag{26}$$

$$\tau_2^{(n)}\left[R\left(v_1^{(n)}\right) + Mg\theta^{(n)} - \overline{T^r}\left(v_1^{(n)}\right)\right] \le 0, \ \ n = 1, 2, \cdots, N \tag{27}$$

Eqs. (19) and (20) require that the initial speed of each stage should be equal to the terminal speed of the previous stage; Eq. (21) defines the speed at the two ends of the journey; Eq. (22) is the speed limit constraint, where the speeds at only the two ends of each operation are confined since the speed is monotonically changing with time during a particular operation (proved in Appendix B); Eq. (23) is the total journey time constraint; Eq. (24) confines the time duration of each operation on each stage, where $S^{(k)} / \overline{v}^{(k)}$ is the lower bound of running time on subsection k; Eq. (25) requires that the sum of the distances traversed during the four stages of each subsection should equal the subsection length; Eqs. (26)-(27) are equivalent to the following feasibility condition of the SH stage,

$$\begin{cases} \tau_2^{(n)} \geq 0, & \text{if } -\overline{B^r}\left(v_1^{(n)}\right) \leq R\left(v_1^{(n)}\right) + Mg\theta^{(n)} \leq \overline{T^r}\left(v_1^{(n)}\right) \\ \tau_2^{(n)} = 0, & \text{otherwise} \end{cases}, \quad n = 1, 2, \cdots, N$$

in other words, the SH operation can be applied if and only if the required tractive/braking force is available.

The following algorithm is used to solve NLP (18)-(27).

Algorithm 1

Step 1: Denote by $U[a,b]$ the uniform distribution on the interval $[a,b]$. The initial values of $v_i^{(n)}$ and $\tau_i^{(n)}$ are generated according to the following rules:

$$v_0^{(n)} \begin{cases} = V_0 & n = 1 \\ \sim U\left[0, \min\left(\bar{v}^{(n-1)}, \bar{v}^{(n)}\right)\right] & n = 2, 3, \cdots, N \end{cases}$$

$$v_1^{(n)} \sim U\left[0, \bar{v}^{(n)}\right], \quad v_2^{(n)} = v_1^{(n)}, \quad v_3^{(n)} \sim U\left[0, \bar{v}^{(n)}\right], \quad n = 1, 2, \cdots, N$$

$$v_4^{(n)} = \begin{cases} v_0^{(n-1)} & n = 1, 2, \cdots, N-1 \\ V_f & n = N \end{cases}$$

$$\rho^{(n)} \sim U[0,1], \quad n = 1, 2, \cdots, N$$

$$\sigma_i^{(n)} \sim U[0,1], \quad n = 1, 2, \cdots, N, \quad i = 1, 2, 3, 4$$

$$\tau_i^{(n)} = \frac{\sigma_i^{(n)}}{\sum_{i=1}^{4} \sigma_i^{(n)}} \times \left[\frac{S^{(n)}}{\bar{v}^{(n)}} + \frac{\rho^{(n)}}{\sum_{n=1}^{N} \rho^{(n)}} \times \left(T - \sum_{k=1}^{N} \frac{S^{(k)}}{\bar{v}^{(k)}}\right)\right]$$

Step 2: The initial values generated from Step 1 are used to solve the following minimisation problem:

$$\min 0 \quad \text{s.t. Eqs. (19)-(27)}$$

Step 3: The solution of Step 2 is used as the initial value to solve NLP (18)-(27).

Remark 3. As we will find later in the case study in Section 5.2, the solution based on the four-stage strategy may contain operations of very short durations, due to either the short length of the corresponding subsection or the limited accuracy of the solver, making the resultant control profiles not easy to directly implement for train driving. Our suggestions for eliminating (part of) these operations are provided as follows.

(I) A short subsection (e.g. 10m, depending on the real situation) can be merged into its adjacent subsection, when the latter has the same gradient but a lower speed limit.

(II) An operation lasts for a very short period of time on a relatively long subsection may (although not always) indicate that such operation is redundant. Therefore, we can remove all of these operations, and then reconstruct and resolve the NLP problem by using the existing solution as the initial value. Generally speaking, within the total $4N$ operations, most of them are actually redundant, so the reconstructed NLP problem will be much easier and faster to solve. The suggested rules for determining which operations to remove are given as follows.

   (i) The first operation (i.e. MT) on the first subsection, and the last operation (i.e. MB) on the last subsection, will never be removed;

   (ii) For each subsection, the operation with the longest time duration will not be removed (to guarantee that at least one operation is applied on each subsection);

   (iii) Operations lasting less than a certain threshold (e.g. 1s, depending on the real situation) will be removed, except those protected by the above two rules.

   It is worth noting that, while attempting to remove the redundant operations, we might have a chance to remove those operations that are necessitated for constructing the optimal solution; however, it would not compromise the optimality too much when the threshold is small. □

3.2. Method 2: constant-force strategy

The four-stage strategy in Section 3.1 requires piecewise-quadratic $\overline{T}^r(v)$ and $\overline{B}^r(v)$ functions. To allow more general forms of these two functions, in this part, we let the train apply constant force when traversing a subsection, so we do not need Assumption 3. By replacing the four-stage strategy with the constant-force strategy, the energy consumption may increase; however, the computation might be faster since the numbers of decision variables and constraints are reduced.

Following Section 3.1, denote by $u^{(n)}$ and $\tau^{(n)}$ the constant applied force and time duration of subsection n, and $\phi_u\left(v_0^{(n)},\tau^{(n)},u^{(n)},\theta^{(n)}\right)$ and $s_u\left(v_0^{(n)},\tau^{(n)},u^{(n)},\theta^{(n)}\right)$ respectively the functions of terminal speed and distance traversed. The optimal train control problem with the constant-force strategy is then formulated as the following NLP.

$$\min_{\left\{v_0^{(n)},\tau^{(n)},u^{(n)}\right\}} \sum_{n=1}^{N} S^{(n)} \max\left\{u^{(n)},0\right\} \tag{28}$$

$$\text{s.t.} \quad v_0^{(n)} = \phi_u\left(v_0^{(n-1)},\tau^{(n-1)},u^{(n-1)},\theta^{(n-1)}\right), \quad n = 2,3,\cdots,N \tag{29}$$

$$v_0^{(1)} = V_0, \quad \phi_u\left(v_0^{(N)},\tau^{(N)},u^{(N)},\theta^{(N)}\right) = V_f \tag{30}$$

$$0 \le v_0^{(n)} \le \min\left\{\overline{v}^{(n-1)},\overline{v}^{(n)}\right\}, \quad n = 2,3,\cdots,N \tag{31}$$

$$\sum_{n=1}^{N} \tau^{(n)} = T \tag{32}$$

$$\frac{S^{(n)}}{\overline{v}^{(n)}} \le \tau^{(n)} \le T - \sum_{k=1,k\ne n}^{N} \frac{S^{(k)}}{\overline{v}^{(k)}}, \quad n = 1,2,\cdots,N \tag{33}$$

$$s_u\left(v_0^{(n)},\tau^{(n)},u^{(n)},\theta^{(n)}\right) = S^{(n)}, \quad n = 1,2,\cdots,N \tag{34}$$

$$-\min\left\{\overline{B^r}\left(v_0^{(n)}\right),\overline{B^r}\left(v_0^{(n+1)}\right)\right\} \le u^{(n)} \le \min\left\{\overline{T^r}\left(v_0^{(n)}\right),\overline{T^r}\left(v_0^{(n+1)}\right)\right\}, \quad n = 1,2,\cdots,N-1 \tag{35}$$

$$-\min\left\{\overline{B^r}\left(v_0^{(n)}\right),\overline{B^r}\left(V_f\right)\right\} \le u^{(n)} \le \min\left\{\overline{T^r}\left(v_0^{(n)}\right),\overline{T^r}\left(V_f\right)\right\}, \quad n = N \tag{36}$$

Eq. (29) requires the initial speed at each subsection equalling the terminal speed of the previous subsection, and Eq. (30) defines the speeds at the two ends of the journey; Eq. (31) is the speed limit constraint, and again the speeds at only the two ends of a subsection are restricted since the speed is monotonically changing with time under a constant force (proved in Appendix B); Eq. (32) is the total journey time constraint; Eq. (33) confines the travel time on each subsection; Eq. (34) is the travel distance constraint; Eqs. (35) and (36) ensure the availability of the applied force, based on the fact that the train speed is monotonically changing with time on each subsection when the applied force is constant.

The following algorithm is used to solve NLP (28)-(36).

Algorithm 2

Step 1: The initial values of $v_0^{(n)}$, $u^{(n)}$ and $\tau^{(n)}$ are generated based on the following rules:

$$v_0^{(n)} \begin{cases} = V_0 & n = 1 \\ \sim U\left[0, \min\left(\overline{v}^{(n-1)},\overline{v}^{(n)}\right)\right] & n = 2,3,\cdots,N \end{cases}$$

$$u^{(n)} \sim \begin{cases} U\left[-\min\left\{\overline{B^r}\left(v_0^{(n)}\right), \overline{B^r}\left(v_0^{(n+1)}\right)\right\}, \min\left\{\overline{F^r}\left(v_0^{(n)}\right), \overline{F^r}\left(v_0^{(n+1)}\right)\right\}\right] & n = 1, 2, \cdots, N-1 \\ U\left[-\min\left\{\overline{B^r}\left(v_0^{(n)}\right), \overline{B^r}\left(V_f\right)\right\}, \min\left\{\overline{F^r}\left(v_0^{(n)}\right), \overline{F^r}\left(V_f\right)\right\}\right] & n = N \end{cases}$$

$$\rho^{(n)} \sim U[0,1], \quad n = 1, 2, \cdots, N$$

$$\tau^{(n)} = \frac{S^{(n)}}{\overline{v}^{(n)}} + \frac{\rho^{(n)}}{\sum_{n=1}^{N} \rho^{(n)}} \times \left(T - \sum_{k=1}^{N} \frac{S^{(k)}}{\overline{v}^{(k)}}\right), \quad n = 1, 2, \cdots, N$$

Step 2: The initial values generated by Step 1 are used to solve the following minimisation problem:

$\min 0$ s.t. Eqs. (29)-(36)

Step 3: The solution of Step 2 is used as the initial value to solve NLP (28)-(36).

Case studies will be provided later in Section 5.2 to compare the performance of the proposed fours-stage and constant-force methods. Before that, we will illustrate how to adopt these two methods in solving the more complex optimal train control problems.

4. Complex optimal train control problems

In this section, we illustrate how to apply the two novel methods that we have just proposed to solve the more complex optimal train control problems about the subway line scheduling (Section 4.1) and the simultaneous optimisation of a leading-following train pair (Section 4.2).

4.1. Energy-efficient subway line scheduling with sophisticated train control

In this part, we show how to calculate the energy-efficient subway line schedules while considering the sophisticated train control, based on the methods proposed in Section 3. We consider the same problem as that in Section 4.2 of Ye and Liu (2016). The subway line has $L+1$ stations, which are sequentially numbered from 1 to $L+1$ along the train's running direction. The track segment between stations l and $l+1$ is defined as section l. Denote $N^{(l)}$ as the total number of subsections on section l, and $Q^{(l)} = \sum_{k=1}^{l} N^{(k)}$, $l \geq 1$, as the total number of subsections on sections 1 to l, and $Q^{(0)} = 0$. The train needs to stop at each station for passenger alighting and boarding. The interstation running time from station l to station $l+1$ is bounded by $\left[T_{min}^{(l)}, T_{max}^{(l)}\right]$, and the total interstation running time from station 1 to station $L+1$ is fixed at T. To find the most energy-efficient schedule and the associated energy-efficient controls, we employ the four-stage strategy and formulate a new mathematical programming problem by adding following additional constraints (37)-(39) to NLP (18)-(27),

$$v_4^{\left(Q^{(l)}\right)} = 0, \quad l = 1, 2, \cdots, L-1 \tag{37}$$

$$V_0 = 0, \quad V_f = 0 \tag{38}$$

$$T_{min}^{(l)} \le \sum_{n=Q^{(l-1)}+1}^{Q^{(l)}} \sum_{i=1}^{4} \tau_i^{(n)} \le T_{max}^{(l)}, \quad l = 1, 2, \cdots, L \tag{39}$$

where Eqs. (37)-(38) specify that the train should have zero speed at both ends of each section, and Eq. (39) constrains the interstation running times. Similarly, with the constant-force strategy, constraints (40)-(42) will be added into NLP (28)-(36).

$$v_0^{\left(Q^{(l)}\right)+1} = 0, \quad l = 1, 2, \cdots, L-1 \tag{40}$$

$$V_0 = 0, \quad V_f = 0 \tag{41}$$

$$T_{min}^{(l)} \le \sum_{n=Q^{(l-1)}+1}^{Q^{(l)}} \tau^{(n)} \le T_{max}^{(l)}, \quad l = 1, 2, \cdots, L \tag{42}$$

A case study will be provided in Section 5.3 for this train scheduling and optimal control problem.

4.2. Optimal control of multiple trains in fixed-block and moving-block signalling systems

In this part, we illustrate how to optimise the control of a leading-following train pair in both fixed-block (Section 4.2.1) and moving-block (Section 4.2.2) signalling systems based on the methods proposed in Section 3. The two trains are numbered 1 and 2, respectively, where train 1 leads train 2. The departure and arrival times (speeds) of train k are respectively denoted by $T_{k,0}$ ($V_{k,0}$) and $T_{k,f}$ ($V_{k,f}$). The functions of maximum tractive force, maximum braking force and resistance of train k are given as $\overline{T_k^r}(\cdot)$, $\overline{B_k^r}(\cdot)$ and $R_k(\cdot)$, respectively.

4.2.1. Fixed-block signalling system

We consider the simplest fixed-block system where no temporary speed limit is applied on the blocks behind the occupied ones. Assume that the track is divided into M block sections which are sequentially numbered 1 to M along the train running direction. Same as Section 4.1, assume that each block section m contains $N^{(m)}$ subsections, and let $Q^{(m)} = \sum_{k=1}^{m} N^{(k)}$ be the total number of subsections on sections 1 to m, and $Q^{(0)} = 0$. A train cannot enter a block until this block is unoccupied for at least a predetermined time of $h \geq 0$.

For the four-stage strategy, denote by $v_{k,0}^{(n)}$ and $t_{k,0}^{(n)}$ the speed and time moment of train k entering subsection n, $v_{k,i}^{(n)}$ and $t_{k,i}^{(n)}$ the speed and time of train k finishing stage i (then $\tau_{k,i}^{(n)} = t_{k,i}^{(n)} - t_{k,i-1}^{(n)}$ is the time duration of stage i) on subsection n, and $\phi_{k,i}\left(v_{k,i-1}^{(n)}, \tau_{k,i}^{(n)}, \theta^{(n)}\right)$ and $s_{k,i}\left(v_{k,i-1}^{(n)}, \tau_{k,i}^{(n)}, \theta^{(n)}\right)$ the functions of terminal speed and distance traversed of train k on stage i on subsection n. Further, let $E_{k,i}\left(v_{k,i-1}^{(n)}, \tau_{k,i}^{(n)}, \theta^{(n)}\right)$, $i = 1, 2$, be the energy consumed by train k during stage i on subsection n. The NLP for minimising the total energy consumption of both trains is then formulated as follows.

$$\min_{\left\{v_{k,i}^{(n)}, t_{k,i}^{(n)}\right\}} \sum_{k=1}^{2} \sum_{n=1}^{N} \sum_{i=1}^{2} E_{k,i}\left(v_{k,i-1}^{(n)}, \tau_{k,i}^{(n)}, \theta^{(n)}\right) \tag{43}$$

$$\text{s.t.} \quad v_{k,i}^{(n)} = \phi_{k,i}\left(v_{k,i-1}^{(n)}, \tau_{k,i}^{(n)}, \theta^{(n)}\right), \quad k = 1, 2, \quad i = 1, 2, 3, 4, \quad n = 1, 2, \cdots, N \tag{44}$$

$$v_{k,0}^{(n)} = v_{k,4}^{(n-1)}, \quad k = 1, 2, \quad n = 2, 3, \cdots, N \tag{45}$$

$$v_{k,0}^{(1)} = V_{k,0}, \quad v_{k,4}^{(N)} = V_{k,f}, \quad k = 1, 2 \tag{46}$$

$$0 \leq v_{k,i}^{(n)} \leq \bar{v}^{(n)}, \quad k = 1, 2, \quad i = 0, 1, 2, 3, \quad n = 1, 2, \cdots, N \tag{47}$$

$$\tau_{k,i}^{(n)} = t_{k,i}^{(n)} - t_{k,i-1}^{(n)}, \quad k = 1, 2, \quad i = 1, 2, 3, 4, \quad n = 1, 2, \cdots, N \tag{48}$$

$$t_{k,0}^{(n)} = t_{k,4}^{(n-1)}, \quad k = 1, 2, \quad n = 2, 3, \cdots, N \tag{49}$$

$$t_{k,0}^{(1)} = T_{k,0}\,,\;\; t_{k,4}^{(N)} = T_{k,f}\,,\;\; k = 1,2 \tag{50}$$

$$0 \le \tau_{k,i}^{(n)} \le T - \sum_{j=1,\, j\ne n}^{N} \frac{S^{(j)}}{\overline{v}^{(j)}}\,,\;\; k = 1,2\,,\;\; i = 1,2,3,4\,,\;\; n = 1,2,\cdots,N \tag{51}$$

$$\sum_{i=1}^{4} s_{k,i}\left(v_{k,i-1}^{(n)}, \tau_{k,i}^{(n)}, \theta^{(n)}\right) = S^{(n)}\,,\;\; k = 1,2\,,\;\; n = 1,2,\cdots,N \tag{52}$$

$$\tau_{k,2}^{(n)}\left[R_k\left(v_{k,1}^{(n)}\right) + Mg\theta^{(n)} + \overline{B_k^r}\left(v_{k,1}^{(n)}\right)\right] \ge 0\,,\;\; k = 1,2\,,\;\; n = 1,2,\cdots,N \tag{53}$$

$$\tau_{k,2}^{(n)}\left[R_k\left(v_{k,1}^{(n)}\right) + Mg\theta^{(n)} - \overline{T_k^r}\left(v_{k,1}^{(n)}\right)\right] \le 0\,,\;\; k = 1,2\,,\;\; n = 1,2,\cdots,N \tag{54}$$

$$t_{2,0}^{\left(Q^{(m-1)}+1\right)} \ge t_{1,4}^{\left(Q^{(m)}\right)} + h\,,\;\; m = 1,2,\cdots,M \tag{55}$$

Constraints (44)-(47) and (51)-(54) are of the same meaning as their counterparts in Eqs. (19) -(22) and (24)-(27); Eq. (48) defines the time duration of each stage; constraints (49)-(50) are similar to constraints (45)-(46); constraint (55) specifies the train separation requirement in the fixed-block system.

The NLP formulation under the constant-force strategy can be easily established by referring to NLP (28)-(36) in Section 3.2 and NLP (43)-(55) above and thus is not explicitly provided here.

4.2.2. Moving-block signalling system

The safe train separation in a moving-block system can be expressed as the minimum headway in either space or time. When neither train changes the operation (MT, SH, CS, MB, or constant force), the two trains' speeds are monotonically changing with time, but neither the distance nor the time headway between them. As a result, the minimum headway is not always achieved at the beginning or end of an operation. However, because our methods only track the train status at the two ends of each operation, we are not able to model the true moving-block system but only an approximate one, which is named by us a "quasi-moving-block system".

Assuming the minimum space headway is d. The max-length SP is first modified according to some $\overline{S}$, as described in Section 2. Consequently, the lengths of the modified subsections will not exceed $\bar{S}$. Now, as illustrated in Figure 3, under the modified SP, given each subsection n which satisfies $X^{(n+1)} - X^{(1)} \geq d$, the subsection $n' = \max\left\{ j \mid X^{(n+1)} - X^{(j)} \geq d,\ j = 1, 2, \cdots, n \right\}$ naturally satisfies $d \leq X^{(n+1)} - X^{(n')} < d + \bar{S}$. If we forbid train 2 to enter subsection n' until train 1 leaves subsection n, then the allowed minimum distance is $X^{(n+1)} - X^{(n')}$. In other words, the allowed minimum space headway along the train journeys is not uniquely d but varies within $\left[d, d + \bar{S} \right)$ with the location of the leading train. Then by choosing a reasonably small $\bar{S}$, we can approximate the true moving-block system without remarkable capacity loss. The NLP for this quasi-moving-block system with the four-stage strategy is formulated as NLP (43)-(54) plus the following train separation constraint (56),

$$t_{2,0}^{(n')} \geq t_{1,4}^{(n)},\quad n' = \max\left\{ j \mid X^{(n+1)} - X^{(j)} \geq d,\ j = 1, 2 \cdots, n \right\},\quad n \in \left\{ j \mid X^{(j+1)} - X^{(1)} \geq d,\ j = 1, 2, \cdots, N \right\} \quad (56)$$

The quasi-moving-block system with constant-force strategy can be formulated in a similar way but again is not provided here.

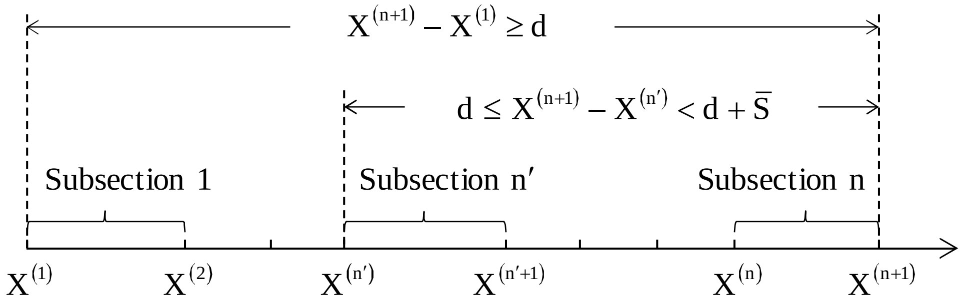

Figure 3. A quasi-moving-block system

5. Case studies

In this part, we examine the performance of the proposed methods in solving practical optimal train control problems based on a subway line which will be introduced in Section 5.1. Section 5.2 compares the two proposed methods and the PM in solving the classic optimal train control problems, and Section 5.3 solves the subway line scheduling and optimal control problem.

The algorithms are all programmed and run in MATLAB R2016a on a desktop computer of 8G RAM and an Intel(R) Core(TM) i5-4460 @ 3.20GHz CPU. The NLP problems based on Methods 1 and 2 are solved by the interior point method with the help of MATLAB's built-in function fmincon, and the parameter values used are listed in Table 1. To use the PM, the optimal train control problems are first formulated as the multiphase optimal control (MOC) problems and then solved by the PM (via discretisation) with the help of GPOPS Version 5.1 (Benson et al., 2006; Garg et al., 2010, 2011a, 2011b; Rao et al., 2010). Details of solving the optimal train control problems by the PM will not be provided in this paper, but interested readers can refer to Wang and Goverde (2016a, 2016b, 2016c), Wang et al. (2013), Ye and Liu (2016), and references therein. Parameter settings of GPOPS are given in Table 2, the explanation of which can be found in Appendix B of Ye and Liu (2016).

Table 1. Parameter settings of fmincon for Methods 1 and 2

Parameter	Method 1 (Algorithm 1)		Method 2 (Algorithm 2)	
	Step 2	Step 3	Step 2	Step 3
'Algorithm'	'interior-point'	'interior-point'	'interior-point'	'interior-point'
'SubproblemAlgorithm'	'factorization'	'cg'	'cg'	'factorization'
'TolX'	1e-14	1e-14	1e-14	1e-14
'TolCon' & 'TolFun'	1e-10	1e-10	1e-10	1e-10
'MaxIter'	4000	4000	4000	4000
'MaxFunEvals'	2e6	2e6	2e6	2e6

Table 2. Parameter settings of GPOPS Version 5.1

Parameter	Column I	Column II
setup.autoscale	'off'	'off'
limits(p).nodesPerInterval	40 (p=1,⋯,27)	30 (p=1,⋯,13)
limits(p).meshPoints	[-1,1] (p=1,⋯,27)	[-1,1] (p=1,⋯,13)
setup.mesh.iteration	0	0
setup.derivatives	'complex'	'complex'
setup.tolerances	[1e-10,1e-10]	[1e-8,1e-8]

5.1. Track and train settings

We use the same track and train settings as that used in Ye and Liu (2016), based on the 22728m-long Yizhuang subway line in Beijing, China, with 14 stations. The station information and practical timetable is given in Table C.1 of Appendix C. The speed limit and track gradient data are given in Table C.2 and Table C.3 of Appendix C, respectively. The train mass is $M = 2.78\times10^5$ kg, and the functions of resistance as well as maximum tractive and maximum braking forces are given below, where v is in km/h, and $R(v)$, $\overline{F^r}(v)$ and $\overline{B^r}(v)$ are in kN.

$$R(v) = 2.2294\times10^{-3}v^2 + 3.9476$$

$$\overline{F^r}(v) = \begin{cases} 310, & 0 \le v \le 36 \\ 310 - 5(v-36), & 36 < v \le 80 \end{cases}$$

$$\overline{B^r}(v) = \begin{cases} 260, & 0 \le v \le 60 \\ 260 - 5(v-60), & 60 < v \le 80 \end{cases}$$

5.2. Comparisons of Method 1, Method 2 and PM for the classic *optimal* train control problem

We drive the train from Songjiazhuang (SJ) to Jiugong (JG) without stopping at the intermediate stations. The train speeds are zero at both ends, and the total journey time is 370 seconds. The optimal train control strategies will be calculated by Methods 1 and 2 and the PM. For Method 1, the max-length SP (Table C.4, Appendix C) is used, which contains 27 subsections. For Method 2, we consider both the max-length SP and three modified subsection plans with $\bar{S}$ of 300m, 200m and 100m, respectively. Thus regarding Methods 1 and 2, we have in total five cases to compare, i.e., Method 1 with max-length SP and Method 2 with four different SPs. For each case, 100 randomly generated initial points are used in Step 1 of Algorithm 1/2 to solve the corresponding optimal train control problem. For the PM, a MOC problem of 27 phases is formulated by associating each subsection with a phase, and the formulation is given in Appendix D. The PM is run only once, and the parameter settings for GPOPS are given in Table 2 (Column I).

The outputs and performance of fmincon and GPOPS are summarised in Table 3. MATLAB’s built-in ODE solver ode45 is further utilized to generate the train speed profiles in Figure 4 and Figure 5, given control profiles suggested by Methods 1 and 2. The speed and control profiles suggested by GPOPS are shown in Figure 6. The results are discussed as follows.

(1) In most cases, Methods 1 and 2 can converge to a feasible solution within the

predetermined tolerance and predetermined number of iterations.

(2) The solution from Method 1 is globally optimal, which is evident based on two reasons. First, different starting points give the almost identical energy consumption (Table 3) and speed profiles (Figure 4). Second, as given in Figure 5 and Table 4, the journey starts with MT and ends with CS followed by MB; while in between, CS and MT are used in turn to adjust the train speed, and SH is used when reaching the speed limit. Such a driving pattern is consistent with the proved optimal train control rule.

(3) For Method 2, only locally optimal solutions are found, which can be told from both the energy consumption (Table 3) and the speed profiles (Figure 4). However, these sub-optimal solutions are neither deviating too much from each other nor very far from the true optimum. With the max-length SP, the computation time of Method 2 is shorter than that of Method 1. As $\bar{S}$ decreases to 200m, the number of subsections almost doubles and the computation time quadruples; however, the energy saving is only slightly improved. When $\bar{S}$ is further shortened by half from 200m to 100m, the energy consumption significantly drops with the increase of subsection number and computation time.

(4) The PM gives almost the same energy consumption (Table 3) and speed profile (except some fluctuation during SH, see Figure 6) as that of Method 1; however, the computation time is much longer (although it depends on the parameter settings), and the fluctuation on the control and speed profiles makes them difficult to follow or implement in the automatic train operating. The cause of the fluctuation during the SH was explained in Ye and Liu (2016), but we would like to restate it here. As we can see, the fluctuation happens at the expected SH operation, which corresponds to the singular arc in the optimal train control problem (Albrecht et al., 2016a; Howlett, 2000; Khmelnitsky, 2000; Liu and Golovitcher, 2003). It is known that the singular arc of an optimal control problem may not be perfectly realised by the so-called direct method including PM, unless the singular arc conditions are explicitly provided in the original optimal control formulation (Betts, 2010; Garg, 2011; Patterson and Rao, 2014; Rao et al., 2010). There are methods (Albrecht et al., 2016a, 2016b; Howlett et al., 2009) for finding such singular SH periods in a classic optimal train control problem; however, it is very difficult, if not impossible, to extend these methods for multiple trains and/or multiple intermediate stations discussed in this paper.

Table 3. Result comparison

		Method 1	Method 2	Method 2	Method 2	Method 2	PM
SP		Max-length	Max-length	$\bar{S}$ =300m	$\bar{S}$ =200m	$\bar{S}$ =100m	Max-length
No. of subsections		27	27	37	46	78	27
Failed trials*		2/100	0/100	1/100	1/100	3/100	-
Computation time (s)	Max**	22.4	24.2	124.2	131.7	458.4	-
	Mean**	16.2	9.6	25.8	36.3	109.6	100
	Min**	11.3	4.2	10.7	17.7	35.1	-
Energy consumption (J/kg)***	Max**	313.1	326.0 (+4.1%)	325.1 (+3.8%)	326.1 (+4.2%)	322.3 (+2.9%)	-
	Mean**	313.1	324.3 (+3.6%)	323.4 (+3.3%)	323.5 (+3.3%)	317.0 (+1.2%)	313.1
	Min**	313.1	324.2 (+3.5%)	323.0 (+3.2%)	323.1 (+3.2%)	316.1 (+1.0%)	-

*A trial fails if a feasible solution cannot be found within prescribed tolerance and prescribed number of iterations.

** The failed trials are excluded.

***The percentages are calculated based on the energy consumption of 313.1J/kg from Method 1.

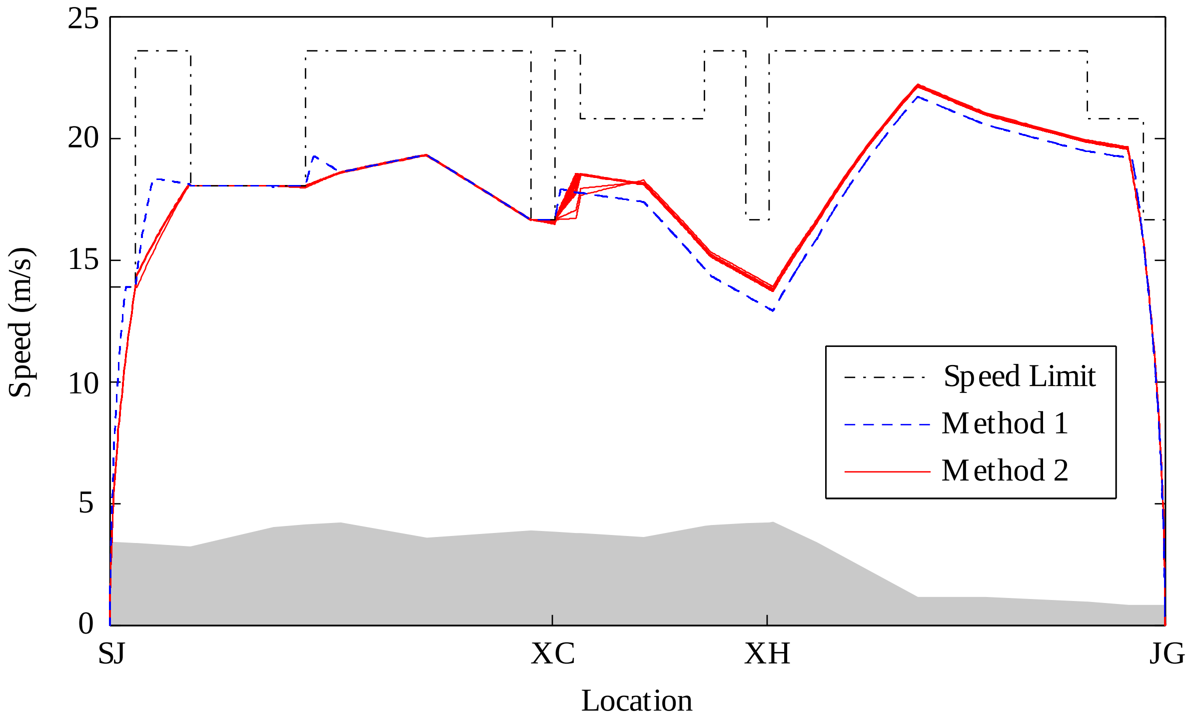

Figure 4. Optimal speed profiles obtained by Methods 1 and 2 with all 100 starting points (excluding failed trials) under the max-length SP (shadowed area illustrating terrain).

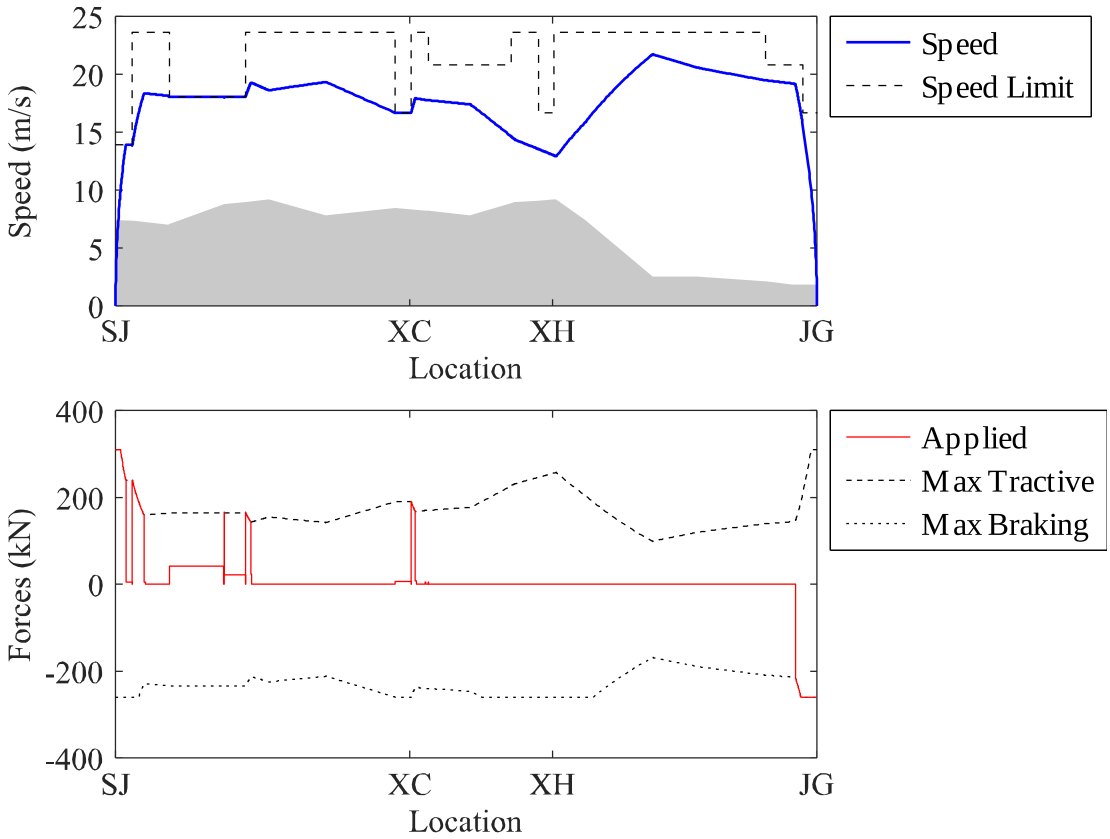

Figure 5. Speed and control profiles obtained by Method 1 with a particular starting point (excluding operations lasting less than 0.01s).

Table 4. Control profile in Figure 5: duration (in second) of each operation on each subsection

Subsection	1	2	3	4	5	6	7	8	9
MT	12.947	0.702	5.724	0.001	0.001	0.080	2.548	0.001	0.000
SH	4.027	0.002	0.817	0.007	26.853	10.423	0.530	0.001	0.005
CS	0.085	0.001	10.980	0.545	0.278	0.073	7.985	26.866	34.487
MB	0.000	0.000	0.000	0.000	0.000	0.000	0.000	0.000	0.000
Subsection	10	11	12	13	14	15	16	17	18
MT	0.000	0.000	2.029	0.001	0.001	0.000	0.000	0.000	0.000
SH	0.008	8.335	0.594	0.113	0.090	0.003	0.001	0.003	0.002
CS	0.052	0.183	4.551	1.404	21.118	22.728	2.480	15.047	10.391
MB	0.000	0.000	0.000	0.000	0.000	0.000	0.000	0.000	0.000
Subsection	19	20	21	22	23	24	25	26	27
MT	0.000	0.000	0.000	0.000	0.000	0.000	0.000	0.000	0.000
SH	0.002	0.000	0.000	0.000	0.001	0.001	0.001	0.000	0.000
CS	1.695	18.036	31.802	18.914	29.959	0.409	12.505	1.444	0.000
MB	0.000	0.000	0.000	0.000	0.000	0.000	0.001	3.612	16.510

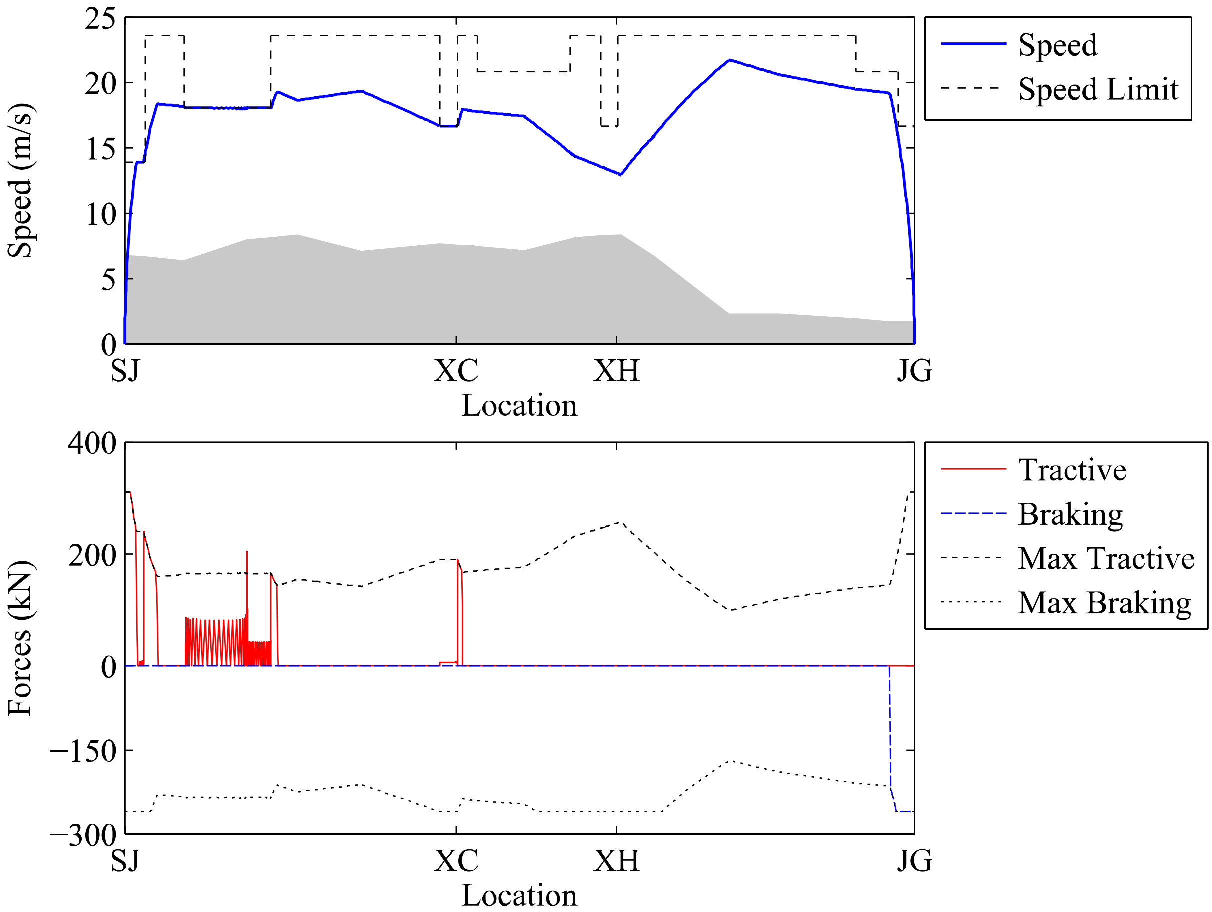

Figure 6. Speed and control profiles obtained by PM.

As one can find from Figure 5 and Table 4, the control profile suggested by Method 1 may contain operations of extremely short durations. We then adopt the technique in Remark 3 to remove operations shorter than 1s, without combining subsections. The new results are listed in Table 5, and for comparison the results of the original Method 1 is duplicated from Table 3 (with one more digit). Clearly, after operation removal, the new NLP is very easy to solve; the energy consumption is slightly improved, which is not surprising since the removed operations are highly likely to be unnecessary. Particularly, the original speed and control profiles in Figure 5 and Table 4 are improved to Figure 7 and Table 6.

Table 5. Result comparison for Method 1

		Original	Some operations removed
SP		Max-length	Max-length
Failed trials		2/100	0/98*
Computation time (s) **	Max	22.42	1.78
	Mean	16.16	0.93
	Min	11.32	0.87

Energy consumption (J/kg) **	Max	313.14	313.11
	Mean	313.13	313.11
	Min	313.13	313.11

*Only the outputs of the successful trials in the original Method 1 are used as the input.
** The failed trials are excluded.

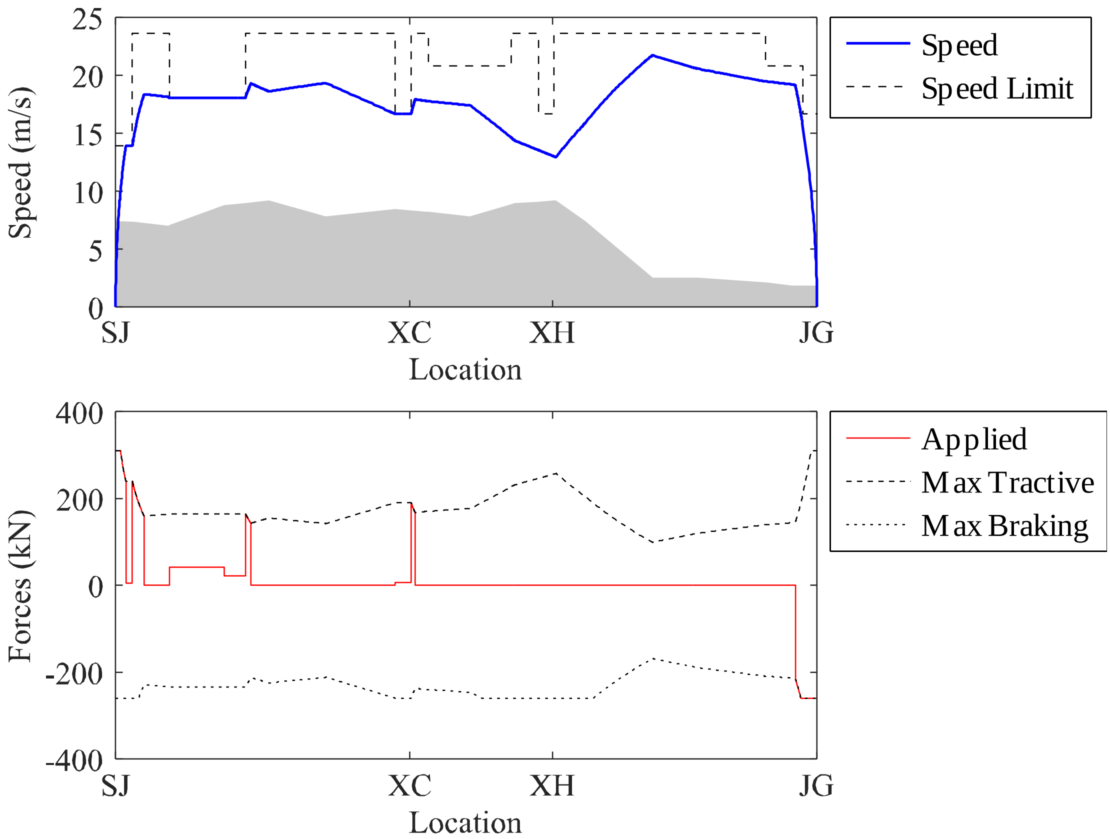

Figure 7. Speed and control profiles obtained by Method 1 (with some operations removed in Figure 5)

Table 6. Control profile in Figure 7: duration (in second) of each operation on each subsection (the blank cells indicating the operations are not applied)

Subsection	1	2	3	4	5	6	7	8	9
MT	12.95	0.70	5.75				2.63		
SH	4.11				27.13	10.58			
CS			11.77	0.55			8.44	26.87	34.49
MB									
Subsection	10	11	12	13	14	15	16	17	18
MT			2.06						
SH		8.52							
CS	0.06		5.11	1.52	21.21	22.73	2.48	15.05	10.39
MB									

Subsection	19	20	21	22	23	24	25	26	27
MT									
SH									
CS	1.70	18.04	31.80	18.92	29.96	0.41	12.51	1.44	
MB								3.61	16.51

5.3. Subway line scheduling and *optimal train* control

As discussed in Ye and Liu (2016), to improve the energy efficiency of the subway line schedule, the PM gave a different schedule from the practical one in use, but the resultant energy consumption was not significantly reduced. Two possible explanations were given for this finding: either the original schedule is already quite energy efficient, or the solution obtained by the PM is only sub-optimal. With the methods proposed in this paper, we now have a chance to identify the true reason(s).

We use Method 1 to calculate the most energy-efficient schedule of the whole Yizhuang line. The bounds of the interstation running times are given in Table 7, which is obtained by introducing ±30s offsets to the original schedule (from Table C.1) on each interstation journey, while taking into account the minimum interstation running time (Table 8). The minimum running time is calculated by replacing the objective function in Eq. (18) with journey time T. The output/performance of Method 1 (based on max-length SP) is summarised in Table 9; the max-length SP here is created by putting together the max-length SPs of all sections, so that the stations are at the ends of the subsections. An identical optimal schedule is obtained and shown in Table 10, where for comparison we also provide the original schedule as well as the optimal schedule obtained by PM. For the PM, the MOC formulation we use here is exactly the one used in Section 4.2 of Ye and Liu (2016), where each interstation journey is associated with a phase; however, we use a different set of parameters in GPOPS (Table 2, Column II) which leads to smaller feasibility and optimality tolerances. Notably, we round the optimised running times to integers while maintaining the total running times to be exactly the same as that of the original schedule. All the three values of the minimum total energy consumption (MTEC) listed in Table 10 is solved by Method 1 (based on max-length SP): given the corresponding schedule, the minimum energy consumption of each interstation journey is calculated by Method 1 and then added up to get the MTEC value. Based on these results, we can answer the question raised in the preceding paragraph. On one hand, the timetable in use is actually quite energy efficient, since the energy saved by Method 1 is very small. On the other hand, the schedule given by PM is more energy-efficient than the practical one but less than the one suggested by Method 1, which means that the PM may not be able to give the globally optimal solution. In fact, it is quite difficult to choose appropriate parameters of GPOPS to ensure the convergence of the programme to a solution within acceptable tolerances; while for Method 1, it is easy to choose the parameters for fmincon to guarantee convergence to an optimal solution in most cases.

Table 7. Lower and upper bounds of interstation running time

Section l	1	2	3	4	5	6	7	8	9	10	11	12	13
$T_{min}^{(l)}$ (s)	160	82	127	110	68	91	80	83	134	122	117	80	84
$T_{max}^{(l)}$ (s)	220	138	187	165	120	144	133	134	194	180	170	132	135

Table 8. Minimum interstation running time

Section l	1	2	3	4	5	6	7	8	9	10	11	12	13
Time (s)	150	82	126	110	68	91	80	83	133	122	117	80	84

Table 9. Results of Method 1

No. of subsections	Failed trials	Computation time (s)			Energy consumption (J/kg)		
		Max	Mean	Min	Max	Mean	Min
101	0/100	249.7	186.0	135.0	2160.8	2160.8	2160.8

Table 10. Schedules and total energy consumption

Schedule	Interstation running time (s)													MTEC (J/kg)
	1	2	3	4	5	6	7	8	9	10	11	12	13	
Original	190	108	157	135	90	114	103	104	164	150	140	102	105	2180.23
Optimal (Method 1)	177	104	150	141	90	118	106	110	156	153	143	105	109	2160.89 (-0.89%*)
Optimal (PM)	174	106	146	140	90	119	105	109	156	152	149	105	111	2164.87 (-0.70%*)

* Compared with the original schedule

6. Conclusions

The traditional optimal train control, which seeks the energy-efficient train-driving strategy under a limited journey time budget, has been well formulated, solved and implemented in real-life train operations. The research now turns to a more complex phase involving multiple trains and/or intermediate constraints, e.g., simultaneously optimising the control of multiple interacting trains, or combining optimal train control with the process of train scheduling. Existing methods all have their limitations and disadvantages in solving these practical problems of interest, which leads us to propose new solution methods in this paper. By assuming that the track is composed of subsections where each subsection has constant speed limit and constant gradient, and that the running resistance is a quadratic function of speed, our proposed two methods adopt two different operating strategies on each subsection, one is a sequence of four stages (MT-SH-CS-MB), and the other is constant force. The four-stage strategy requires the maximum tractive and maximum braking forces taking the decreasing and piecewise-quadratic form w.r.t. speed, while the constant-force strategy only requires decreasingness. For each of the five operations (MT, SH, CS, MB, and constant force), given its initial speed and time duration, we calculated the closed-form expressions of its terminal speed, travel distance and energy consumption. Based on these closed-form expressions, we formulated and solved the optimal train control problems as the NLP problems. Such NLP formulations were then used to solve the problems of energy-efficient train scheduling along a multi-station subway line, as well as the optimal control of a leading-following train pair under both fixed-block and moving-block signalling systems. A case study showed the difference of the two proposed methods in computational efficiency and solution optimality for solving a classic single-train single-journey optimal control problem, where the PM was also included for comparison. Another case study demonstrated the effectiveness of the proposed method in solving a practical subway line scheduling problem.

The merits of the proposed methods lie in their effectiveness and efficiency in solving the complex optimal train control problems, as well as the ease in implementing the advised controls. The four-stage strategy will be able to yield the optimal train control since the MT-SH-CS-MB sequence has been proved to be energy-efficient under constant speed limit and constant gradient. The requirement of this strategy on the forms of maximum tractive and maximum braking forces may restrict its usage when facing more general forms of these two forces; however, such obstacle is not insuperable since the more complex force forms can always be approximated by piecewise-linear or piecewise-quadratic functions. Alternatively, the constant-force strategy allows more general forms of maximum tractive and maximum braking forces, and according to our case study it can achieve a stable and satisfying level of energy saving.

For future research, it is still attractive to develop the indirect methods based on Pontryagin's maximum principle for the complex problems that are discussed in this paper. Meanwhile, as mentioned in Haahr et al. (2017), with the intermediate time-window (and speed-window) constraints, only one sequence of MT-SH-CS-MB on each subsection could be non-optimal or even infeasible; therefore, it is important to see how our Method 1 can be adapted to this scenario. We also notice that the dynamic programming method in Haahr et al. (2017) is efficient in solving the single-train optimal control problems with intermediate time constraints; however, their method on generating speed profiles is based on simulation or numerical methods, so there is scope for their process to be speeded up by using the closed-form expressions we used in this paper. Last but not least, it is also interesting to use the method in Haahr et al. (2017) for the optimal control of multiple trains.

Acknowledgement

The authors wish to express their thanks to the Associate Editor Dr Xuesong Zhou and four anonymous reviewers for their useful comments on earlier versions of this paper. The work described in this paper was supported by the UK Rail Safety and Standards Board, Grant No. T1071.

Appendix A. Closed-form expressions of speed, distance and energy

In this appendix, we calculate the closed-form solution to the general ODE

$$\frac{dv}{dt} = av^2 + bv + c, \quad a \neq 0, \quad v(t_0) = v_0 \tag{A.1}$$

Notably, only the key processes rather than all the tedious details will be provided. Since $a \neq 0$, we let $w = v + b/(2a)$ and rewrite Eq. (A.1) as

$$\frac{dw}{dt} = a\left(w^2 + \frac{4ac - b^2}{4a^2}\right), \quad a \neq 0, \quad w(t_0) = w_0 = v_0 + \frac{b}{2a} \tag{A.2}$$

Defining $X = \sqrt{|4ac - b^2|}/(2a)$, the ODE in Eq. (A.2) can be further transformed as follows.

(1) If $4ac - b^2 = 0$ and $w_0 = 0$, then $dw/dt = 0$;

(2) If $4ac - b^2 = 0$ and $w_0 \neq 0$, then $dw/w^2 = a\,dt$;

(3) If $4ac - b^2 > 0$, then $dw/(w^2 + X^2) = a\,dt$;

(4) If $4ac - b^2 < 0$ and $|w_0| = |X|$, then $dw/dt = 0$;

(5) If $4ac - b^2 < 0$ and $|w_0| \neq |X|$, then $dw/(w^2 - X^2) = a dt$, which further writes $dw/(w - X) - dw/(w + X) = 2aX dt$.

The closed-form expression of $v(t)$ under each of the five scenarios above is calculated and provided in Table A.1, based on which the distance traversed $\int_{t_0}^{t} v(t) dt$ and the integral $\int_{t_0}^{t} (v(t))^2 dt$ for calculating the energy consumption are also calculated.

Remark A.1. From Table A.1, when $4ac - b^2 > 0$, since the $\tan(\cdot)$ function is undefined at $\pm\pi/2$, t should satisfy $aX(t - t_0) + z \in (-\pi/2, \pi/2)$. This constraint is difficult to be, and thus is not, included in our NLP formulations. Therefore, the optimal train control profiles, once obtained, should be further checked against this constraint. All results in the case studies of this paper satisfy this constraint; however, occasionally in other scenarios, faulty results which violate this constraint were spotted. □

Table A.1. Closed-form expressions of speed, distance traversed, and integral of square of speed

Condition	Speed $v(t)$	Distance traversed $\int_{t_0}^{t} v(t)\,dt$	$\int_{t_0}^{t} (v(t))^2\,dt$
$4ac-b^2=0$ & $v_0=-b/(2a)$	v_0	$v_0(t-t_0)$	$v_0^2(t-t_0)$
$4ac-b^2=0$ & $v_0\neq-b/(2a)$	$\dfrac{1}{-a(t-t_0)+\dfrac{2a}{2av_0+b}}-\dfrac{b}{2a}$	$-a\ln\left\|1-\left(av_0+\dfrac{b}{2}\right)(t-t_0)\right\|-\dfrac{b}{2a}(t-t_0)$	$\dfrac{1}{a^2}\left(\dfrac{1}{\dfrac{2}{2av_0+b}-(t-t_0)}-\dfrac{1}{\dfrac{2}{2av_0+b}}\right)+\dfrac{b}{a^2}\ln\left\|\dfrac{2av_0+b}{2}(t-t_0)-1\right\|+\left(\dfrac{b}{2a}\right)^2(t-t_0)$
$4ac-b^2>0$	$X\tan(aX(t-t_0)+z)-\dfrac{b}{2a}$ where $z=\arctan\left(\dfrac{v_0}{X}+\dfrac{b}{2aX}\right)$, and $aX(t-t_0)+z\in\left(-\dfrac{\pi}{2},\dfrac{\pi}{2}\right)$	$-\dfrac{1}{a}\ln\left\|\dfrac{\cos(aX(t-t_0)+z)}{\cos(z)}\right\|-\dfrac{b}{2a}(t-t_0)$	$\dfrac{X}{a}\tan(aX(t-t_0)+z)+\dfrac{b}{a^2}\ln\left\|\dfrac{\cos(aX(t-t_0)+z)}{\cos(z)}\right\|+\left[\left(\dfrac{b}{2a}\right)^2-X^2\right](t-t_0)-\dfrac{1}{a}\left(v_0+\dfrac{b}{2a}\right)$
$4ac-b^2<0$ & $v_0=\pm X-b/(2a)$	v_0	$v_0(t-t_0)$	$v_0^2(t-t_0)$
$4ac-b^2<0$ & $v_0\neq\pm X-b/(2a)$	$\dfrac{2X}{1-y\exp[2aX(t-t_0)]}-\dfrac{b}{2a}-X$ where $y=\dfrac{2a(v_0-X)+b}{2a(v_0+X)+b}$	$-\dfrac{1}{a}\ln\left\|\dfrac{1-y\exp[2aX(t-t_0)]}{1-y}\right\|+\left(X-\dfrac{b}{2a}\right)(t-t_0)$	$\dfrac{2X}{a}\left(\dfrac{1}{1-y\exp[2aX(t-t_0)]}-\dfrac{1}{1-y}\right)+\dfrac{b}{a^2}\ln\left\|\dfrac{1-y\exp[2aX(t-t_0)]}{1-y}\right\|+\left(X-\dfrac{b}{2a}\right)^2(t-t_0)$

Appendix B. Switching condition in the MT and MB stages

According to Table A.1, the derivative of $v(t)$ writes

$$\frac{dv}{dt}=\begin{cases}0 & 4ac-b^2=0, v_0=-b/(2a)\\ \dfrac{a}{\left[a(t-t_0)-\dfrac{2a}{2av_0+b}\right]^2} & 4ac-b^2=0, v_0\neq -b/(2a)\\ aX^2\left[1+\tan^2\left(aX(t-t_0)+\arctan\left(\dfrac{v_0}{X}+\dfrac{b}{2aX}\right)\right)\right] & 4ac-b^2>0\\ 0 & 4ac-b^2<0, v_0=\pm X-b/(2a)\\ \dfrac{4aX^2\dfrac{2a(v_0-X)+b}{2a(v_0+X)+b}\exp\left[2aX(t-t_0)\right]}{\left\{1-\dfrac{2a(v_0-X)+b}{2a(v_0+X)+b}\exp\left[2aX(t-t_0)\right]\right\}^2} & 4ac-b^2<0, v_0\neq \pm X-b/(2a)\end{cases} \tag{B.1}$$

which means the speed changes monotonically during each particular operation. Denoting t^c as the value such that $v(t^c)=v^c$, then generally speaking, the maximum tractive/braking force will switch (i) from the low-speed regime to the high-speed regime only if the speed is increasing and $t>t^c$, and (ii) from the high-speed regime to the low-speed regime only if the speed is decreasing and $t>t^c$. Mathematically, the switching happens if and only if one of the following six conditions hold.

(I) $4ac-b^2=0$, $v_0\neq -\dfrac{b}{2a}$, $t>t^c=t_0+2\left(\dfrac{1}{2av_0+b}-\dfrac{1}{2av^c+b}\right)$, and

(i) $v_0<v^c$ and $a>0$ (switching from Regime 1 to 2); or

(ii) $v_0>v^c$ and $a<0$ (switching from Regime 2 to 1).

(II) $4ac-b^2>0$, $t>t^c=t_0+\dfrac{1}{aX}\left[\arctan\left(\dfrac{v^c}{X}+\dfrac{b}{2aX}\right)-\arctan\left(\dfrac{v_0}{X}+\dfrac{b}{2aX}\right)\right]$, and

(i) $v_0<v^c$ and $a>0$ (switching from Regime 1 to 2); or

(ii) $v_0 > v^c$ and $a < 0$ (switching from Regime 2 to 1).

(III) $4ac - b^2 < 0$, $v_0 \neq \pm X - \frac{b}{2a}$, $\frac{2a(v_0 + X) + b}{2a(v_0 - X) + b} \frac{2a(v^c - X) + b}{2a(v^c + X) + b} > 0$,

$t > t^c = t_0 + \frac{1}{2aX} \ln\left[\frac{2a(v_0 + X) + b}{2a(v_0 - X) + b} \frac{2a(v^c - X) + b}{2a(v^c + X) + b}\right]$, and

(i) $v_0 < v^c$ and $a \frac{2a(v_0 - X) + b}{2a(v_0 + X) + b} > 0$ (switching from Regime 1 to 2); or

(ii) $v_0 > v^c$ and $a \frac{2a(v_0 - X) + b}{2a(v_0 + X) + b} < 0$ (switching from Regime 2 to 1).

Appendix C. Line and operation information of the Yizhuang line

Table C.1. Station location and practical timetable of the Yizhuang line

Station No.	Station Name	Location (m)	Arrival (s)	Departure (s)	Dwell (s)
1	Songjiazhuang (SJ)	0	-	0	-
2	Xiaocun (XC)	2631	190	220	30
3	Xiaohongmen (XH)	3905	328	358	30
4	Jiugong (JG)	6271	515	545	30
5	Yizhuangqiao (YZQ)	8254	680	715	35
6	Wenhuayuan (WH)	9246	805	835	30
7	Wanyuan (WY)	10785	949	979	30
8	Rongjing (RJ)	12065	1082	1112	30
9	Rongchang (RC)	13419	1216	1246	30
10	Tongjinan (TJ)	15756	1410	1440	30
11	Jinghai (JH)	18021	1590	1620	30
12	Ciqunan (CQN)	20107	1760	1795	35
13	Ciqu (CQ)	21394	1897	1942	45
14	Yizhuang (YZ)	22728	2047	-	-

Table C.2. Speed limit (SL) in the form: SL ($km \cdot h^{-1}$)/start location (m) - end location (m)

50/0-150	85/150-480	65/480-1161	85/1161-2501	60/2501-2643	85/2643-2797
75/2797-3534	85/3534-3780	60/3780-3918	85/3918-5808	75/5808-6141	60/6141-6281
85/6281-8122	60/8122-8265	85/8265-9116	60/9116-9259	85/9259-10655	60/10655-10797
85/10797-11933	60/11933-12077	85/12077-13289	60/13289-13431	85/13431-14649	70/14649-15426
85/15426-15624	60/15624-15768	85/15768-17891	60/17891-18033	85/18033-19982	60/19982-20120
85/20120-21264	60/21264-21406	85/21406-22569	60/22569-22728		

Table C.3. Track gradient in the form: gradient (‰)/start location (m) - end location (m)

-2/0-160	-3/160-470	10.4/470-970	3/970-1370	-8/1370-1880	3/1880-2500
-2/2500-2770	-3/2770-3170	8.2/3170-3570	2/3570-3940	-20.4/3940-4200	-24/4200-4800
0/4800-5200	-2/5200-5800	-3.2/5800-6050	0/6050-6370	3.3/6370-6770	2.8/6770-7150
-15.6/7150-7415	9/7415-7675	0/7675-8376	5/8376-8736	-2/8736-9036	0/9036-9366
-2/9366-9806	5/9806-10126	3/10126-10606	0/10606-10866	2/10866-11426	-3/11426-11826
0/11826-12116	3.5/12116-12736	-1.8/12736-13116	0/13116-13526	-0.5/13526-13926	1.5/13926-14546
-1/14546-15176	6/15176-15476	0/15476-16006	-8/16006-16326	-3/16326-16696	5/16696-17136
1.4/17136-17816	0/17816-18136	15.5/18136-18486	24/18486-19186	-3/19186-19426	10.1/19426-19776
2/19776-20121	-3/20121-20796	3/20796-21231	2/21231-21481	20/21481-21681	3/21681-22066
-18.9/22066-22416	2/22416-22728				

Table C.4. Max-length SP for case study in Section 5.2

Subsection No.	1	2	3	4	5	6	7	8	9	10	11	12	13	14
Start (m)	0	150	160	470	480	970	1161	1370	1880	2500	2501	2643	2770	2797
End (m)	150	160	470	480	970	1161	1370	1880	2500	2501	2643	2770	2797	3170
SL (km/h)	50	85	85	85	65	65	85	85	85	85	60	85	85	75
Gradient (‰)	-2	-2	-3	10.4	10.4	3	3	-8	3	-2	-2	-2	-3	-3
Subsection No.	15	16	17	18	19	20	21	22	23	24	25	26	27	
Start (m)	3170	3534	3570	3780	3918	3940	4200	4800	5200	5800	5808	6050	6141	
End (m)	3534	3570	3780	3918	3940	4200	4800	5200	5800	5808	6050	6141	6271	
SL (km/h)	75	85	85	60	85	85	85	85	85	85	75	75	60	
Gradient (‰)	8.2	8.2	2	2	2	-20.4	-24	0	-2	-3.2	-3.2	0	0	

Appendix D. The MOC formulation used in Section 5.2 for solving the classic optimal train control problem

In this appendix, we provide the MOC formulation used in Section 5.2 for solving the classic single-train optimal control by the PM. Similar to Wang and Goverde (2016a), we associate each subsection with a phase, therefore the resultant MOC problem for a train journey passing N subsections will have N phases. The independent variable is time. Denote $t_0^{(p)}$ / $x_0^{(p)}/v_0^{(p)}$ and $t_f^{(p)}/x_f^{(p)}/v_f^{(p)}$ respectively as the start and end time/location/speed of a phase p, i.e., the time/location/speed of entering and leaving a subsection p. Meanwhile, let $x^{(p)}\left(t^{(p)}\right)$, $v^{(p)}\left(t^{(p)}\right)$, $T_r^{(p)}\left(t^{(p)}\right)$ and $B_r^{(p)}\left(t^{(p)}\right)$ respectively be the location, speed, applied tractive force and applied braking force at time $t^{(p)}$ during phase p. Then the classic single-train optimal control problem (1)-(9) is reformulated to be a MOC problem as follows.

$$\min \sum_{p\in\mathbb{P}} \int_{t_0^{(p)}}^{t_f^{(p)}} T_r^{(p)}(t) v^{(p)}(t) dt, \quad \mathbb{P} = \{1, 2, \cdots, N\}$$

subject to the dynamic constraints

$$\frac{dx^{(p)}}{dt^{(p)}} = v^{(p)}, \quad p \in \mathbb{P}$$

$$\frac{dv^{(p)}}{dt^{(p)}} = \frac{1}{M}\left[T_r^{(p)} - B_r^{(p)} - R\left(v^{(p)}\right) - Mg\theta^{(p)}\right], \quad p \in \mathbb{P}$$

the boundary conditions

$$t_0^{(1)} = 0, \quad t_f^{(N)} = T$$

$$x\left(t_0^{(p)}\right) = X^{(p)}, \quad x\left(t_f^{(p)}\right) = X^{(p+1)}, \quad p \in \mathbb{P}$$

$$v\left(t_0^{(1)}\right) = V_0, \quad v\left(t_f^{(N)}\right) = V_f$$

$$\frac{S^{(p)}}{\overline{v}^{(p)}} \le t_f^{(p)} - t_0^{(p)} \le T - \sum_{i=1, i\ne p}^{N} \frac{S^{(i)}}{\overline{v}^{(i)}}, \quad p \in \mathbb{P}$$

the path constraints

$$0 \le v^{(p)} \le \overline{v}^{(p)}, \quad T_r^{(p)} \ge 0, \quad T_r^{(p)} - \overline{T^r}\left(v^{(p)}\right) \le 0, \quad B_r^{(p)} \ge 0, \quad B_r^{(p)} - \overline{B^r}\left(v^{(p)}\right) \le 0, \quad p \in \mathbb{P}$$

and the linkage constraints

$$t_f^{(p)} = t_0^{(p+1)}, \quad v_f^{(p)} = v_0^{(p+1)}, \quad p \in \mathbb{P} \setminus \{N\}$$

References

Açıkbaş, S., Söylemez, M.T., 2008. Coasting point optimisation for mass rail transit lines using artificial neural networks and genetic algorithms. IET Electric Power Applications 2 (3), 172-182.

Albrecht, A.R., Howlett, P.G., Pudney, P.J., Vu, X., Zhou, P., 2015. Energy-efficient train control: The two-train separation problem on level track. Journal of Rail Transport Planning & Management 5 (3), 163-182.

Albrecht, A., Howlett, P., Pudney, P., Vu, X., Zhou, P., 2016a. The key principles of optimal train control-Part 1: Formulation of the model, strategies of optimal type, evolutionary lines, location of optimal switching points. Transportation Research Part B 94, 482-508.

Albrecht, A., Howlett, P., Pudney, P., Vu, X., Zhou, P., 2016b. The key principles of optimal train control-Part 2: Existence of an optimal strategy, the local energy minimization principle, uniqueness, computational techniques. Transportation Research Part B 94, 509-538.

Asnis, I.A., Dmitruk, A.V., Osmolovskii, N.P., 1985. Solution of the problem of the energetically optimal control of the motion of a train by the maximum principle. USSR Computational Mathematics and Mathematical Physics 25 (6), 37-44.

Benson, D.A., Huntington, G.T., Thorvaldsen, T.P., Rao, A.V., 2006. Direct trajectory optimization and costate estimation via an orthogonal collocation method. Journal of Guidance, Control, and Dynamics 29 (6), 1435-1440.

Betts, J., 2010. Practical Methods for Optimal Control and Estimation using Nonlinear Programming. Society for Industrial and Applied Mathematics.

Chang, C.S., Sim, S.S., 1997. Optimising train movements through coast control using genetic algorithms. IEE Proceedings - Electric Power Applications 144 (1), 65-73.

Cheng, J., Davydova, Y., Howlett, P., Pudney, P., 1999. Optimal driving strategies for a train journey with non-zero track gradient and speed limits. IMA Journal of Management Mathematics 10 (2), 89-115.

Cheng, J., Howlett, P., 1992. Application of critical velocities to the minimisation of fuel consumption in the control of trains. Automatica 28 (1), 165-169.

Cheng, J., Howlett, P., 1993. A note on the calculation of optimal strategies for the minimization of fuel consumption in the control of trains. IEEE Transactions on Automatic Control 38 (11), 1730-1734.

Chevrier, R., Pellegrini, P., Rodriguez, J., 2013. Energy saving in railway timetabling: A bi-objective evolutionary approach for computing alternative running times. Transportation Research Part C 37, 20-41.

Das Gupta, S., Tobin, J.K., Pavel, L., 2016. A two-step linear programming model for energy-efficient timetables in metro railway networks. Transportation Research Part B 93, 57-74.

Davis, W.J., 1926. The tractive resistance of electric locomotives and cars. General Electric Review 29 (10), 685-707.

Effati, S., Roohparvar, H., 2006. The minimization of the fuel costs in the train transportation. Applied Mathematics and Computation 175 (2), 1415-1431.

Franke, R., Terwiesch, P., Meyer, M., 2000. An algorithm for the optimal control of the driving of trains. Proceedings of the 39th IEEE Conference on Decision and Control, 2000, vol.3, pp. 2123-2128.

Garg, D., 2011. Advances in Global Pseudospectral Methods for Optimal Control. PhD Thesis. University of Florida.

Garg, D., Hager, W.W., Rao, A.V., 2011a. Pseudospectral methods for solving infinite-horizon optimal control problems. Automatica 47 (4), 829-837.

Garg, D., Patterson, M., Francolin, C., Darby, C., Huntington, G., Hager, W., Rao, A., 2011b. Direct trajectory optimization and costate estimation of finite-horizon and infinite-horizon optimal control problems using a Radau pseudospectral method. Computational Optimization and Applications 49 (2), 335-358.

Garg, D., Patterson, M., Hager, W.W., Rao, A.V., Benson, D.A., Huntington, G.T., 2010. A unified framework for the numerical solution of optimal control problems using pseudospectral methods. Automatica 46 (11), 1843-1851.

Goodwin, J.C.J., Fletcher, D.I., Harrison, R.F., 2016. Multi-train trajectory optimisation to maximise rail network energy efficiency under travel-time constraints. Journal of Rail and Rapid Transit 230 (4), 1318-1335.

Gu, Q., Tang, T., Cao, F., Song, Y.D., 2014. Energy-efficient train operation in urban rail transit using real-time traffic information. IEEE Transactions on Intelligent Transportation Systems 15 (3), 1216-1233.

Haahr, J.T., Pisinger, D., Sabbaghian, M., 2017. A dynamic programming approach for optimizing train speed profiles with speed restrictions and passage points. Transportation Research Part B 99, 167-182.

Howlett, P., 1990. An optimal strategy for the control of a train. The ANZIAM Journal 31 (04), 454-471.

Howlett, P., 1996. Optimal strategies for the control of a train. Automatica 32 (4), 519-532.

Howlett, P., 2000. The optimal control of a train. Annals of Operations Research 98 (1-4), 65-87.

Howlett, P., 2016. A new look at the rate of change of energy consumption with respect to journey time on an optimal train journey. Transportation Research Part B 94, 387-408.

Howlett, P.G., Cheng, J., 1997. Optimal driving strategies for a train on a track with continuously varying gradient. The ANZIAM Journal 38 (03), 388-410.

Howlett, P.G., Pudney, P.J., Vu, X., 2009. Local energy minimization in optimal train control. Automatica 45 (11), 2692-2698.

Ichikawa, K., 1968. Application of optimization theory for bounded state variable problems to the operation of train. Bulletin of JSME 11 (47), 857-865.

Jaekel, B., Albrecht, T., 2014. Comparative analysis of algorithms and models for train running simulation. Journal of Rail Transport Planning & Management 4 (1-2), 14-27.

Khmelnitsky, E., 2000. On an optimal control problem of train operation. IEEE Transactions on Automatic Control 45 (7), 1257-1266.

Ko, H., Koseki, T., Miyatake, M., 2004. Application of dynamic programming to the optimization of the running profile of a train. Computers in Railways IX, WIT Press, 103-112.

Li, X., Lo, H.K., 2014a. An energy-efficient scheduling and speed control approach for metro rail operations. Transportation Research Part B 64, 73-89.

Li, X., Lo, H.K., 2014b. Energy minimization in dynamic train scheduling and control for metro rail operations. Transportation Research Part B 70, 269-284.

Li, S., Yang, L., Gao, Z., 2015. Coordinated cruise control for high-speed train movements based on a multi-agent model. Transportation Research Part C 56, 281-292.

Li, S., Yang, L., Li, K., Gao, Z., 2014. Robust sampled-data cruise control scheduling of high speed train. Transportation Research Part C 46, 274-283.

Liu, R., Golovitcher, I.M., 2003. Energy-efficient operation of rail vehicles. Transportation Research Part A 37 (10), 917-932.

Lu, Q., Feng, X., 2011. Optimal control strategy for energy saving in trains under the four-aspect fixed autoblock system. Journal of Modern Transportation 19 (2), 82-87.

Milroy, I.P., 1980. Aspects of Automatic Train Control. PhD Thesis, Loughborough University.

Patterson, M.A., Rao, A.V., 2014. GPOPS-II: A Matlab software for solving multiple-phase optimal control problems using hp-adaptive Gaussian quadrature collocation methods and sparse nonlinear programming. ACM Transactions on Mathematical Software 41 (1), 1-37.

Pudney, P., Howlett, P., 1994. Optimal driving strategies for a train journey with speed limits. The ANZIAM Journal 36 (01), 38-49.

Rao, A.V., Benson, D.A., Darby, C., Patterson, M.A., Francolin, C., Sanders, I., Huntington, G.T., 2010. Algorithm 902: GPOPS, A MATLAB software for solving multiple-phase optimal control problems using the Gauss pseudospectral method. ACM Transactions on Mathematical Software. 37 (2), 22:1-22:39.

Rochard, B.P., Schmid, F., 2000. A review of methods to measure and calculate train resistances. Journal of Rail and Rapid Transit 214 (4), 185-199.

Scheepmaker, G.M., Goverde, R.M., Kroon, L.G., 2017. Review of energy-efficient train control and timetabling. European Journal of Operational Research 257 (2), 355-376.

Vasak, M., Baotic, M., Peric, N., Bago, M., 2009. Optimal rail route energy management under constraints and fixed arrival time. 2009 European Control Conference (ECC), pp. 2972-2977.

Wang, P., Goverde, R.M.P., 2016a. Multiple-phase train trajectory optimization with signalling and operational constraints. Transportation Research Part C 69, 255-275.

Wang, P., Goverde, R.M., 2016b. Train trajectory optimization of opposite trains on single-track railway lines. 2016 IEEE International Conference on Intelligent Rail Transportation (ICIRT), pp. 23-31.

Wang, P., Goverde, R.M., 2016c. Two-train trajectory optimization with a green-wave policy. Transportation Research Record 2546, 112-120.

Wang, Y., De Schutter, B., van den Boom, T.J.J., Ning, B., 2013. Optimal trajectory planning for trains - A pseudospectral method and a mixed integer linear programming approach. Transportation Research Part C 29, 97-114.

Wang, Y., De Schutter, B., van den Boom, T.J.J., Ning, B., 2014. Optimal trajectory planning for trains under fixed and moving signaling systems using mixed integer linear programming. Control Engineering Practice 22, 44-56.

Wong, K.K., Ho, T.K., 2004. Dynamic coast control of train movement with genetic algorithm. International Journal of Systems Science 35 (13-14), 835-846.

Yan, X., Cai, B., Ning, B., ShangGuan, W., 2016. Online distributed cooperative model predictive control of energy-saving trajectory planning for multiple high-speed train movements. Transportation Research Part C 69, 60-78.

Yang, L., Li, K., Gao, Z., Li, X., 2012. Optimizing trains movement on a railway network. Omega 40 (5), 619-633.

Yang, X., Chen, A., Li, X., Ning, B., Tang, T., 2015. An energy-efficient scheduling approach to improve the utilization of regenerative energy for metro systems. Transportation Research Part C 57, 13-29.

Yang, X., Chen, A., Ning, B., Tang, T., 2016a. A stochastic model for the integrated optimization on metro timetable and speed profile with uncertain train mass. Transportation Research Part B 91, 424-445.

Yang, X., Li, X., Ning, B., Tang, T., 2016b. A survey on energy-efficient train operation for urban rail transit. IEEE Transactions on Intelligent Transportation Systems 17 (1), 2-13.

Ye, H., Liu, R., 2016. A multiphase optimal control method for multi-train control and scheduling on railway lines. Transportation Research Part B 93, 377-393.

Yin, J., Tang, T., Yang, L., Gao, Z., Ran, B., 2016. Energy-efficient metro train rescheduling with uncertain time-variant passenger demands: An approximate dynamic programming approach. Transportation Research Part B 91, 178-210.

Zhou, L., Tong, L.C., Chen, J., Tang, J., Zhou, X., 2017. Joint optimization of high-speed train timetables and speed profiles: A unified modelling approach using space-time-speed grid networks. Transportation Research Part B 97, 157-181.